Functional Characteristics of the Parallel SI- and SII-Projecting Neurons of the Thalamic Ventral Posterior Nucleus in the Marmoset

H. Q. ZHANG, G. M. MURRAY, G. T. COLEMAN, A. B. TURMAN, S. P. ZHANG, AND M. J. ROWE
School of Physiology and Pharmacology, The University of New South Wales, Sydney, NSW 2052, Australia

Received 7 January 2000; accepted in final form 22 January 2001

Zhang, H. Q., G. M. Murray, G. T. Coleman, A. B. Turman, S. P. Zhang, and M. J. Rowe. Functional characteristics of the parallel SI- and SII-projecting neurons of the thalamic ventral posterior nucleus in the marmoset. *J Neurophysiol* 85: 1805–1822, 2001. The functional organization of the primate somatosensory system at thalamocortical levels has been a matter of controversy, in particular, over the extent to which the primary and secondary somatosensory cortical areas, SI and SII, are organized in *parallel* or *serial* neural networks for the processing of tactile information. This issue was investigated for the marmoset monkey by recording from 55 single tactile-sensitive neurons in the lateral division of the ventral posterior nucleus of the thalamus (VPL) with a projection to either SI or SII, identified with the use of the antidromic collision technique. Neurons activated from the hand and distal forearm were classified according to their peripheral source of input and characterized in terms of their functional capacities to determine whether the *direct* thalamic input can account for tactile processing in *both* SI *and* SII. Both the SI- and SII-projecting samples contained a *slowly adapting* (SA) class of neurons, sensitive to static skin displacement, and purely dynamically sensitive tactile neurons that could be subdivided into two classes. One was most sensitive to high-frequency (≥100 Hz) cutaneous vibration whose input appeared to be derived from Pacinian sources, while the other was sensitive to lower frequency vibration (≤100 Hz) or trains of rectangular mechanical pulse stimuli, that appeared to receive its input from *rapidly adapting* (RA) afferent fibers presumed to be associated with intradermal tactile receptors. There appeared to be no systematic differences in functional capacities between SI- and SII-projecting neurons of each of these three classes, based on receptive field characteristics, on the form of stimulus-response relations, and on measures derived from these relations. These measures included threshold and responsiveness values, bandwidths of vibrational sensitivity, and the capacity for responding to cutaneous vibrotactile stimuli with phase-locked, temporally patterned impulse activity. The analysis indicates that low-threshold, high-acuity tactile information is conveyed *directly* to both SI and SII from overlapping regions within the thalamic VP nucleus. This direct confirmation of a parallel functional projection to both SI and SII in the marmoset is consistent with our separate studies at the cortical level that demonstrate *first*, that tactile responsiveness in SII largely survives the SI inactivation and *second*, that SI responsiveness is largely independent of SII. It therefore reinforces the evidence that SI and SII occupy a hierarchically equivalent network for tactile processing.

INTRODUCTION

The primary and secondary somatosensory areas of the cerebral cortex (SI and SII, respectively) constitute two of the principal tactile processing areas in the cortex of most mammalian species (for reviews see Burton 1986; Johnson 1990; Jones 1986; Kaas 1987; Rowe 1990). As both these areas receive direct anatomical projections from the ventral posterior (VP) thalamic nucleus (see Jones 1985), it has usually been assumed that SI and SII were involved in parallel processing of tactile sensory information derived from this thalamic source of input (Mountcastle 1986; Rowe 1990). Direct experimental support for the parallel processing scheme has been presented for several mammalian species, in particular for the cat (Burton and Robinson 1987; Manzoni et al. 1979; Turman et al. 1992, 1995), the rabbit (Murray et al. 1992), the tree shrew, and the prosimian galago (Garraghty et al. 1991), and for a marsupial representative, the possum (Coleman et al. 1999), based on the observation that SI inactivation, achieved with a variety of methods in these species, has little effect on tactile responsiveness within the SII area of cortex.

However, for simian primates, the organization of thalamocortical tactile systems is much less clear. First, it has been reported in both macaque and marmoset monkeys that neurons within the forelimb region of SII became unresponsive to stimulation of this body region following surgical ablation of the topographically related region of SI (Burton et al. 1990; Garraghty et al. 1990b; Pons et al. 1987, 1992). This result was interpreted as evidence for a *serial* or *hierarchical* organizational scheme in which tactile processing within SII is dependent on inputs traversing an indirect, serial, path from the thalamus to SII via SI (Garraghty et al. 1990b; Pons et al. 1987, 1992). Furthermore, in terms of this tactile processing, it was argued that in the marmoset, "SII can be seen as only distantly related to the thalamus" and is "primarily involved in processing information from other cortical fields" (Garraghty et al. 1990b). The findings obtained in support of the serial scheme of processing in the primate species led at that time to the hypothesis that there were fundamental differences between simian primates and nonprimate mammals in the organization of thalamocortical systems for tactile processing (Garraghty et al. 1990b; Murray et al. 1992; Turman et al. 1992).

However, these investigations of the serial/parallel processing hypothesis entailed substantial methodological differences between the studies undertaken in primates and those done on nonprimate species. In particular, the inactivation of SI in the macaque and marmoset monkeys was based on surgical ablation, whereas for the cat and rabbit studies a reversible inactivation procedure based on local anesthetic blockade or localized cortical cooling of SI was

Address reprint requests to M. J. Rowe (E-mail: M.Rowe@unsw.edu.au).

The costs of publication of this article were defrayed in part by the payment of page charges. The article must therefore be hereby marked "*advertisement*" in accordance with 18 U.S.C. Section 1734 solely to indicate this fact.

 0022-3077/01 $5.00 Copyright © 2001 The American Physiological Society

Downloaded from http://jn.physiology.org/ by 10.220.33.4 on September 27, 2016

employed (Burton and Robinson 1987; Murray et al. 1992; Turman et al. 1992, 1995). As the SI ablation procedure is clearly irreversible and does not permit examination of responsiveness in individual SII neurons before, during, and after SI inactivation, we recently re-investigated SII responsiveness in one of the simian primates, the marmoset (*Callithrix jacchus*), when SI inactivation was brought about by the rapid reversible method based on localized cortical cooling. In contrast to the earlier observations with surgical ablation of SI, we found that >90% of SII neurons activated by tactile inputs from the hand and forearm remained responsive to controlled tactile stimulation during SI inactivation (Rowe et al. 1996; Zhang et al. 1996). We speculated that the different result may be attributable to the surgical ablation procedure setting up an injury discharge in corticocortical neurons that project from SI to the topographically related region of SII, which may, in turn, lead to changes in extracellular ion concentrations, in particular, K^+ ion accumulation, and accommodation block of neurons within this region of SII. This hypothesis is based on documented increases in extracellular potassium concentration in brain and spinal cord regions in response to tetanic stimulation of peripheral inputs (Lux and Neher 1973; Vyskočil et al. 1972) and the effects of such increases on transmitter release (Katz and Miledi 1967), membrane potentials (Orkland et al. 1966), and Na^+ channel inactivation (Hodgkin and Huxley 1952) (for further discussion of the effects of extracellular K^+ ion accumulation, see O'Mara et al. 1988).

Our observations that tactile inputs in the marmoset can reach SII directly from the thalamus without traversing an indirect serial path through SI are consistent with a known anatomical projection from the VP thalamic nucleus to SII as well as to SI in simian primates (Brysch et al. 1990; Friedman and Murray 1986; for reviews, see Burton 1986; Jones 1985; Kaas 1987; Steriade et al. 1997). However, it had been proposed that the projection to SII was from the ventral posterior inferior (VPI) nucleus while that to SI arose from the ventral posterolateral (VPL) nucleus (Garraghty et al. 1990b; and see Friedman and Murray 1986; Krubitzer and Kaas 1992). Furthermore, it was argued that the VPI component of VP derived its major input from the spinothalamic tract and was less concerned with low-threshold tactile inputs than were the VPL neurons that projected to SI (Krubitzer and Kaas 1992).

To explore further the controversial issue of the extent to which inputs from low-threshold tactile afferent sources are conveyed directly from VP to SI and SII over parallel projection pathways, we have employed, in the present study, electrophysiological recording from single tactile neurons of the marmoset VP thalamus to examine the functional properties of identified, SI- and SII-projecting thalamocortical neurons. Preliminary accounts of the results have been reported in abstract form (Zhang et al. 1995).

METHODS

Animal preparation

The experiments were performed in 22 adult marmosets (*Callithrix jacchus*) of either sex (230–410 g body wt). All experiments conformed with the Australian Code of Practice for the Care and Use of Animals for Scientific Purposes, the National Institutes of Health Guide for the Care and Use of Laboratory Animals, and the Guiding Principles in the Care and Use of Animals approved by the Council of the American Physiological Society. Anesthesia was induced with intramuscular injection of ketamine (25 mg/kg) and xylazine (2 mg/kg), and maintained by intravenous infusion of ketamine ($\sim$20 mg $\cdot$ $kg^{-1} \cdot h^{-1}$) mixed with xylazine ($\sim$1 mg $\cdot$ $kg^{-1} \cdot h^{-1}$) in 0.18% sodium chloride containing 4% dextrose. The infusion rate was adjusted depending on anesthetic level as evaluated by the autonomic indexes of blood pressure and heart rate, in particular, and by tests for the presence of the flexion reflex. Atropine sulfate (0.08 mg/kg) was administered subcutaneously at the time of anesthesia induction, to reduce respiratory secretions. Dexamethasone phosphate (Decadron, 1.5 mg/kg im) was routinely given to minimize the risk of brain edema. Dextran 40 (Gentran 40, 10% in normal saline, iv) was used in some experiments to maintain satisfactory blood pressure and cerebral circulation. Rectal temperature was maintained at 38 $\pm$ 0.5°C. Other details of the animal preparation were described in our earlier study of SI-SII organization in the marmoset (Zhang et al. 1996). For some animals used in the present thalamic study, anesthesia was maintained for a further 12- to 18-h period, during which an investigation of the response properties of tactile afferent fibers was conducted (Coleman et al. 2001). At the end of the experiment, an overdose of sodium pentobarbitone was administered.

Identification of the SI and SII hand areas

A frontoparietal craniotomy was performed, the dura removed, and a skin pool was filled with warm ($\sim$38°C) paraffin liquid to prevent drying of the exposed cortex. The cerebral cortex was mapped electrophysiologically to determine the foci of the hand representation in SI and SII. These were identified as the areas where short-latency, positive-going evoked potentials were elicited by tap stimuli (3–5 ms, 400- to 800-μm amplitude) applied to the central palm of the contralateral hand that had been fixed in a perspex trough to stabilize the hand and allow accurate positioning of the mechanical stimulator (for details, see Zhang et al. 1996).

Recording and stimulation procedures

Lacquered tungsten microelectrodes (impedance 3–8 MΩ at 1 kHz) were advanced by means of a stepping microdrive through the parietal cortex into the VP thalamus according to stereotaxic coordinates (Stephan et al. 1980). In each track, the cortical surface reading was noted to specify the depth at which each neuron was studied. Extracellular recordings were made from individual neurons that were identified initially from their response to gentle tapping or stroking of the hand or distal forearm. The receptive fields of individual neurons were mapped on the glabrous or hairy skin of the hand and forearm by means of von Frey hairs.

The activity recorded by the microelectrode was amplified, filtered, and passed to a discriminator unit from which constant-output pulses could be relayed to a counter unit and laboratory computer along with appropriate stimulus timing pulses. Output from the preamplifier unit was also passed to an audio amplifier and loudspeaker, and recorded on magnetic tape. The mechanosensitivity of thalamic neurons activated from the hand and forearm was examined with the use of precise and reproducible mechanical stimuli derived from the servo-controlled mechanical stimulator described in the preceding paper (Coleman et al. 2001).

Functional classification and analysis of responsiveness for thalamic tactile neurons

Individual tactile-sensitive thalamic neurons were tested for their responsiveness to a steady rectangular indentation of the skin (applied in a ramp-and-hold form lasting 1–1.5 s and 0.1–1 mm in amplitude).

Downloaded from http://jn.physiology.org/ by 10.220.33.4 on September 27, 2016

This permitted the functional classification of neurons into two broad groups, the slowly adapting (SA) neurons that displayed a sustained response to the steady indentation, and the dynamically sensitive neurons that were responsive to just the ON and OFF phases of the ramp-and-hold stimulus (Bennett et al. 1980; Ghosh et al. 1992; Mountcastle et al. 1969; Zhang et al. 1996). The purely dynamically sensitive tactile neurons were further classified according to their responsiveness to vibrotactile stimuli (see RESULTS).

Impulse rates in the responses of single thalamic neurons to step indentations and vibrotactile stimulation of the skin were counted using a Schmitt trigger unit, and stimulus-response relations constructed by plotting the mean response (to 5–10 stimulus repetitions) as the number of impulses occurring over 1 s against the step indentation amplitude or the peak-to-peak vibration amplitude. The 5–10 repetitions of the vibration stimulus (a 1-s train superimposed on a background 1.5-s step indentation) were used to construct cycle histograms (CHs) and *phase scatter* graphs to analyze the temporal relations between the impulse activity in the thalamic neuron and the vibrotactile stimulus waveform, and to compare quantitatively the capacities of SI- and SII-projecting neurons to respond with phase-locked, patterned impulse activity to the vibration stimuli. The CHs used a pulse associated with the onset of each vibration cycle as the stimulus marker and reflect the probability of impulse occurrence throughout the period of the vibration cycle (Alloway et al. 1988; Ferrington and Rowe 1980a; Mountcastle et al. 1969; Rose et al. 1967; Rowe et al. 1996; Turman et al. 1992; Zhang et al. 1996).

A quantitative measure of phase locking in the responses to vibration, *percentage entrainment*, was calculated as the highest number of impulses in any continuous half-cycle of the CH, expressed as a percentage of the total number of impulses. This measure ranges from a theoretical minimum of 50% (see Ferrington and Rowe 1980a; Zhang et al. 1996), where there is an absence of phase preference in the response and the histogram has a rectangular form, to a maximum of 100%, where all impulses fall within one continuous half-cycle segment of the vibration cycle period. The phase scatter graphs (Figs. 7 and 8) display the time (or phase) of impulse occurrence within the vibration cycle period against the time within the overall 1-s long train of skin vibration (Mackie et al. 1998).

Antidromic identification of SI- and SII-projecting thalamic neurons

The SI and SII areas of hand representation were identified with evoked potential recording in order to place bipolar silver ball electrodes on the cortical surface over the center of each of these cortical regions for the antidromic identification of SI- and SII-projecting thalamic neurons. A third pair of bipolar electrodes was usually placed over the face area of representation that separates the SI and SII hand areas. This was employed for circumstances in which a thalamic neuron was activated by stimulation of *both* the SI and SII hand areas, to determine whether activation from both areas might be attributed to stimulus spread or to genuine bifurcation of the axonal projection to both SI and SII.

Bipolar stimuli used for antidromic testing were up to 10 mA in strength and 50–120 μs in duration and were derived from an isolated pulse stimulator (A-M Systems, model 2100). The majority of neurons studied (55 of 90; >60%; see RESULTS) met the following criteria as thalamo-cortical projection neurons. First, they were characterized by a short, invariant latency (<1.5 ms for all neurons) even when the cortical stimulus strength was near threshold. Second, the cortically evoked spike recorded in the thalamic neuron underwent collision and extinction by prior orthodromic spikes that had been generated by peripheral stimulation. The *collision period* lasted for twice the latency (or conduction time, T) for the cortically induced spike ($2T$) plus a short additional period corresponding to the refractory period ($R \sim$ 0.5 ms) for the axon; that is, a collision period of $2T + R$ (Darian-Smith et al. 1963; Waldron et al. 1989). Third, in only a small proportion of cases (7 neurons), the thalamic neuron was tested and demonstrated to have the capacity to follow high-frequency (>100–200 Hz) cortical stimulation. However, this criterion was not routinely used as Darian-Smith et al. (1963) have pointed out that high-frequency following may permit "no clear differentation of antidromically and *trans*-synaptically induced discharges." As concluded by Fuller and Schlag (1976), "the collision test still probably remains the safest electrophysiological tool for determining the antidromic nature of a unitary response."

Histological verification of recording sites

In selected electrode penetrations, normally at the end of experiments, lesions were made by passing negative current (10–30 mA, 10–30 s) through the tip of the microelectrode at known depths to assist in the identification of neuron locations in subsequent histological examination of sections taken through this region of thalamus. In some experiments, the recording electrode was cut and kept in the last penetration at known stereotaxic coordinates for the same purpose.

At the end of an experiment, the animal was killed by an overdose of sodium pentobarbitone. A block of the thalamus and overlying cortex was collected and fixed in 10% formaline in normal saline, cut into coronal sections of 75-μm thickness on a freezing microtome and stained with cresyl violet. Classification of thalamic nuclei was based on a stereotaxic atlas of the marmoset brain by Stephan et al. (1980).

RESULTS

Classification of SI- and SII-projecting thalamocortical neurons

Ninety neurons with tactile receptive fields located, in all but one case, on the contralateral distal forelimb were isolated for single neuron recording in the thalamus. Most were located 3–5 mm lateral and 3–5 mm rostral to the stereotaxic zero point (Stephan et al. 1980) at a depth of 7–11 mm from the cortical surface. Of the 90 neurons, 55 were shown by means of the antidromic collision technique to have direct projections to the hand areas of SI *or* SII (Table 1). The remaining 35 neurons that could not be activated antidromically from the hand focus of SI or SII are not considered further. The locations within the thalamus of the neurons sampled are described in a later section of RESULTS. Of the 55 identified thalamocortical neurons, 11 projected to SII and 44 projected to SI (Table 1). None could be antidromically activated from *both* SI and SII at stimulus strengths that provided evidence for the presence of a bifurcating thalamocortical projection from individual thalamic neurons to *both* SI and SII in the marmoset.

The antidromic latencies for the two groups were 0.68 ± 0.21 ms (mean ± SD, $n = 28$) for SI-projecting neurons and

TABLE 1. *Functional types of thalamic neurons projecting to SI or SII*

Type	SI	SII
SA	4	3
RA and related	28	1
PC	4	5
HFA	2	0
Other	6	2
Total	44	11

SI and SII, primary and secondary somatosensory cortical areas; SA, slowly adapting; RA, rapidly adapting; PC, Pacinian corpuscle; HFA, hair follicle afferent.

Downloaded from http://jn.physiology.org/ by 10.220.33.4 on September 27, 2016

0.66 ± 0.15 ms ($n = 8$) for SII-projecting neurons, values that were not significantly different ($P = 0.43$). As the path length from VP to the hand representation area of SI and SII is essentially the same (average path length, ~8.5 mm in each case), these latency values convert to mean conduction velocities of 12.5 and 12.9 m/s, respectively.

Of the 11 SII-projecting thalamic neurons, 8 had receptive fields on the glabrous skin of the contralateral hand and could be activated by von Frey hairs of <0.5 g wt force. Two others responded best when the contralateral distal forelimb was manipulated or tapped, or activated by von Frey hairs >0.5 g wt in force and may have had deep input from the distal forelimb (i.e., muscle, tendon, or joint). The remaining neuron had a large cutaneous receptive field on both hairy and glabrous skin of the distal hindlimb. The thalamic neurons with tactile receptive fields on the distal forelimb that projected to SI displayed similar tactile sensitivity to their counterparts that projected to SII, in having von Frey thresholds below 0.5 g wt in all cases and <100 mg wt in 70% of neurons. Furthermore, the functional classification of the 55 thalamocortical neurons (Table 1) demonstrated that the major classes of tactile neuron were represented in *both* the SI- and SII-projecting groups, although the proportions in each projection group differed. Both groups contained SA tactile neurons that displayed sustained responses throughout 1- to 1.5-s steady indentations of the skin, and purely dynamically sensitive neurons that responded to just the ON and OFF phases of the ramp-and-hold indentations.

Among the SI-projecting tactile neurons were 4 SA neurons, representing ~10% of the sample (4/44 neurons), and among SII-projecting neurons there were 3 SA neurons out of a total of 11 neurons (Table 1). Dynamically sensitive neurons constituted the majority of both samples and could be subdivided according to their sensitivity to vibration stimuli by applying earlier criteria for classifying thalamic and cortical tactile neurons (Bennett et al. 1980; Burton 1986; Ghosh et al. 1992; Mountcastle et al. 1969; Turman et al. 1992). Almost all dynamically sensitive tactile neurons had receptive fields that were confined to the glabrous skin of the hand or that included both glabrous and adjacent hairy skin.

One class whose cortical counterpart we have identified previously (Zhang et al. 1996) was designated rapidly adapting (RA), as these neurons were sensitive to low-frequency (<100 Hz) vibration or trains of rectangular mechanical pulse stimuli. Their peripheral input is presumed to come from the RA (or QA, quickly adapting) afferent fibers thought to be associated with intradermal encapsulated receptors of the Meissner or, in the case of the cat, Krause types (Ferrington and Rowe 1980b; Iggo and Ogawa 1977; Jänig 1971; Jänig et al. 1968; Talbot et al. 1968; and see Coleman et al. 2001). Neurons that were unresponsive to sinusoidal vibration but responded to low-frequency (10 Hz) trains of rectangular mechanical pulses were thought to be less-sensitive representatives of the broader RA class of tactile neurons. This broad RA class represented a high proportion (>60%) of the SI-projecting thalamic neurons (28/44 neurons) but was poorly represented among the small sample of SII-projecting neurons (1/11 neurons; Table 1).

Both SI- and SII-projecting groups contained neurons that were most sensitive to high-frequency (>100 Hz), low-amplitude vibration, indicative of an input derived from Pacinian corpuscle (PC) sources in the hand (Burton and Sinclair 1990, 1991; Ferrington and Rowe 1980a,b; Hunt 1961; Talbot et al. 1968; Turman et al. 1992; Zhang et al. 1996). These made up a small proportion (~10%) of the SI-projecting neurons (4/44 neurons) but constituted almost one-half the SII-projecting neuron (5/11 neurons; Table 1).

Both groups also contained a small proportion of rather insensitive tactile neurons (designated "other" in Table 1), making up 15% for SI-projecting and ~20% for SII-projecting neurons. These responded only to tapping or manipulation of the marmoset's hand, or to >2 g wt von Frey hair stimulation and may have been associated with "deep" inputs, perhaps from muscle, joint, or tendon sources in the distal forearm. None of these was studied systematically. Two further neurons in the sample of 55 thalamocortical units studied had their input confined to hair follicle afferent (HFA) fibers and were SI projecting.

The functional classification of the thalamocortical projecting neurons establishes that all classes of tactile neurons activated from the glabrous skin of the marmoset hand are represented, although in different proportions, among *both* the SI- and SII-projecting sample of neurons (Table 1).

Functional capacities of SA SI- and SII-projecting thalamic neurons

The capacity for sustained, or SA responses to static skin displacement (lasting 1–1.5 s) was apparent in both SI- and SII-projecting thalamic neurons as demonstrated by the sample impulse trace records in Figs. 1*A* and 2*A*, respectively. Among seven neurons of the slowly adapting class, four projected to SI and three to SII. In Fig. 1, the response level (in imp/s) was similar in the three illustrated responses of an SI-projecting neuron to static skin displacements of 300, 800, and 1,500 μm, as the neuron displayed an abrupt increase in response level as indentation intensity increased from 100 to 300 μm (—, Fig. 1*B*). The stimulus-response relation for a second SI-projecting neuron (– – –, Fig. 1*B*) also rose to an approximate plateau level of response over an indentation range of <500 μm.

The stimulus-response relation plotted as the continuous line in Fig. 2*B* also shows a steep rise in response level over an ~500-μm range of indentation for the SII-projecting neuron whose response traces are illustrated in Fig. 2*A*. However, the second stimulus-response relation for a different SII-projecting neuron (– – –, Fig. 2*B*) displays a more gradual rise and therefore a broader dynamic range, defined as the range of stimulus intensities over which the neuron exhibited graded responsiveness.

The data in Figs. 1 and 2 show that the stimulus-response relations for thalamocortical neurons of the SA class display some variation from one neuron to another. However, there was no evidence for a systematic difference between the SI- and SII-projecting neurons of this class in the general form of the relations or in any response parameters derived from these relations. For example, all four SA neurons whose stimulus-response relations are illustrated in Figs. 1 and 2 had thresholds to static skin displacement of approximately ≤200 μm. In addition, although the slope over the steepest part of the stimulus-response relations varied from one SA neuron to another over the range ~50–150 impulses s^{-1} mm^{-1}, there was no systematic distinction between SI- and SII-projecting samples. There also appeared to be no systematic distinction

Downloaded from http://jn.physiology.org/ by 10.220.33.4 on September 27, 2016

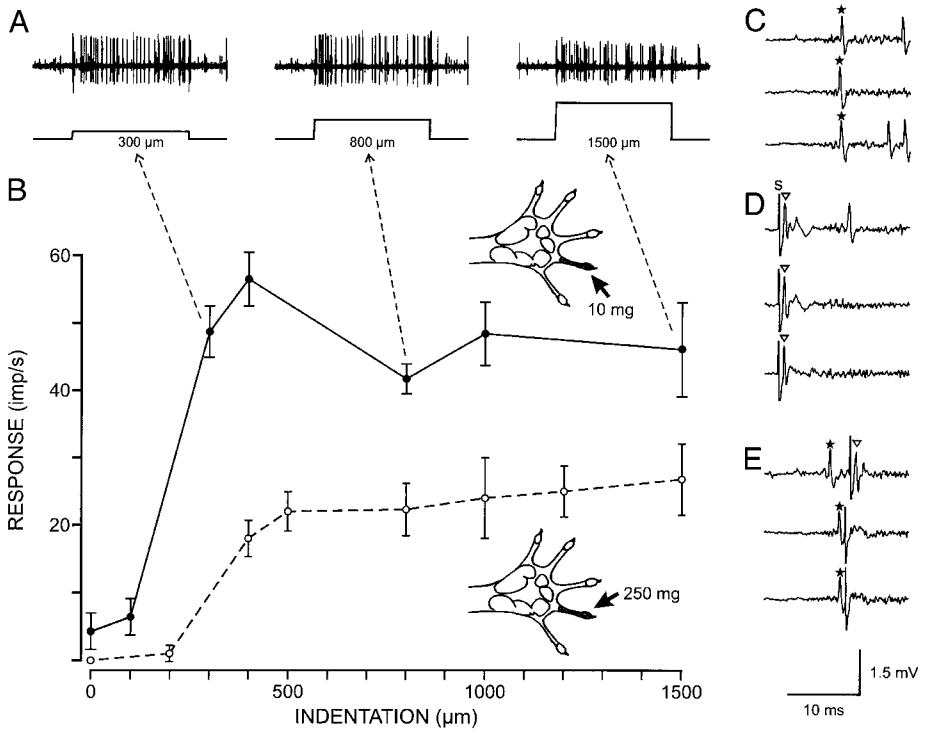

FIG. 1. Response data from a slowly adapting (SA) thalamocortical neuron that projected to the primary somatosensory cortical area (SI). The impulse traces in *A* show the responses of the neuron to 3 intensities of 1.5-s skin indentation (300, 800, and 1,500 μm, respectively, from *left* to *right*), applied to the receptive field on the 4th finger (*top figurine* in *B*). In *B*, the *top graph* plots the response levels (mean ± SD in imp/s, calculated for the initial 1-s skin indentation, $n = 10$) as a function of stimulus intensity. Each arrow points to sample responses obtained at that indentation intensity. The *bottom plot* in *B* shows data from another SA thalamocortical neuron that projected to SI (receptive field in *bottom figurine*). Evidence is provided in *C–E* for a projection to SI for the SA neuron whose responses are shown in *A*. In *C*, the neuron responded (⋆) at a latency of ~10 ms to a skin tap stimulus (800 μm amplitude, 4 ms duration) applied at the onset of each trace. In *D*, an electrical stimulus (S; 3 mA, 120 μs) applied to the SI hand area consistently activated the neuron (▽) at short latency (0.7 ms). In *E*, *top trace*, the neuron responded 1st (⋆) to the peripheral stimulus and then (▽) to the later SI electrical stimulus. As the cortical stimulus was brought closer to the peripherally evoked spikes in the *bottom 2 traces* in *E*, it failed to elicit a response because of collision, demonstrating that the neuron projected to SI.

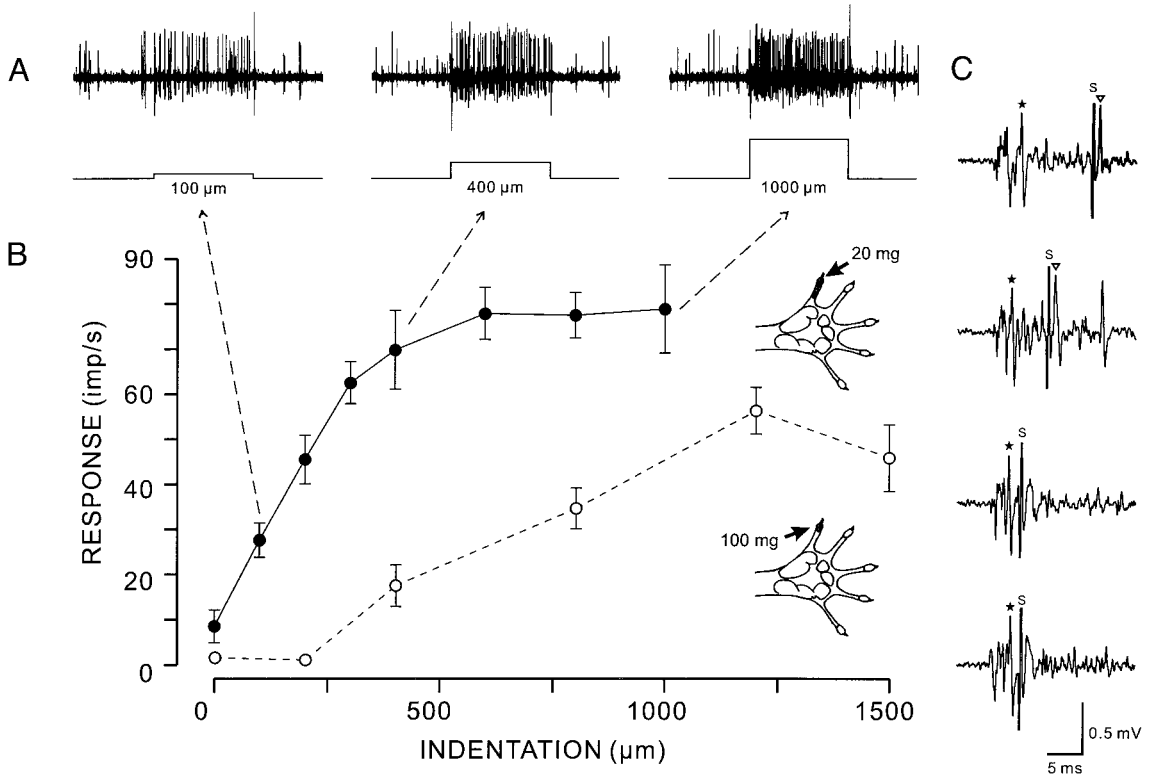

FIG. 2. Response data from a SA thalamocortical neuron that projected to SII. This neuron had a small receptive field on the glabrous skin of the contralateral thumb and could be activated by a 20 mg wt von Frey hair (*top figurine* in *B*). Impulse traces in *A* show the responses of the neuron to 3 intensities of 1-s static skin indentation (100, 400, and 1,000 μm, respectively, from *left* to *right*) and those in *C* and *D*, the evidence for a projection to SII. *B*: stimulus-response relations for 2 SII-projecting SA neurons (format details as in Fig. 1). In *C*, the neuron responded at a latency ~9 ms (⋆) to a brief (~1 ms) tap applied to the contralateral thumb 4 ms prior to the onset of the traces followed by the later SII electrical stimulus (S; 3 mA, 100 μs) that evoked a short-latency (0.7 ms) response (▽). As the cortical stimulus was brought closer to the peripherally evoked spikes in *D*, it failed to elicit a response because of collision, demonstrating that the neuron projected to SII.

Downloaded from http://jn.physiology.org/ by 10.220.33.4 on September 27, 2016

between the two groups in the maximum discharge rates (~25–75 imp/s) attained in the relations.

The receptive field properties in terms of location, size, and threshold for activation by hand-held probes were also comparable between the SI- and SII-projecting SA neurons. For example, the SI-projecting neurons associated with Fig. 1 had small receptive fields on the fourth finger and had different sensitivities; the neuron whose relation is plotted at the *top* of Fig. 1*B* (—) could be activated by a 10-mg von Frey hair, while the other (– – –) required ≥250 mg for activation. The thresholds for activation by von Frey hairs for the other two SI-projecting neurons were 10 and 100 mg. The three SII-projecting SA neurons also had small receptive fields, each of which was restricted to one finger, and von Frey thresholds ranging from 20 to 100 mg.

Evidence for either the SI- or SII-projection target for individual thalamocortical SA neurons came from the collision of antidromic spikes (▽, Figs. 1 and 2), elicited by electrical stimulation (S) of the identified hand areas of SI (Fig. 1, *C–E*) or SII (Fig. 2*C*), with orthodromic spikes (★) generated by skin stimulation. In Fig. 1, *C–E,* the orthodromic spikes for the SI-projecting neuron were evoked at a latency of ~10 ms by a 4-ms, 800-μm amplitude tap stimulus (Fig. 1*C*) and the antidromic spikes at a latency of ~0.7 ms after a 3-mA, 120-μs stimulus (S in Fig. 1, *D* and *E*) to the SI hand area. When the SI stimulus was delivered at ~2 ms or more after the orthodromic spike (*top trace* in *E*), it continued to generate a short-latency response from the thalamic neuron, but failed to do so when it was moved in time so that the interval between the two spikes was below ~2.2 ms, corresponding to the collision period, made up of twice the latency for the thalamic response to the cortical stimulus (2 × 0.7 ms) plus a component attributable to the refractory period of the thalamocortical terminals (~0.7 ms). If the cortical-induced response had been *trans*-synaptically generated, the minimum interval between orthodromic and cortically generated spikes should have been much less, corresponding to the refractory period of the thalamic neuron itself. Similar collision data are presented to establish the antidromic nature of the SII-generated response for the thalamocortical SA neuron of Fig. 2.

Functional capacities of SI- and SII-projecting thalamic neurons of the RA class

This class of thalamocortical neuron, as indicated above (Table 1), was differentially represented among the SI- and SII-projecting groups, with a high incidence among SI-projecting neurons but a sparse representation in the SII-projecting group. This precluded any systematic comparison of the functional characteristics of RA neurons projecting to the two cortical targets. Nevertheless, the characteristics of the identified SII-projecting neuron in this class (Fig. 4) was consistent with those of the large sample of SI-projecting RA neurons. These were responsive to low-frequency sinusoidal vibration (Fig. 3) or to low-frequency rectangular pulse trains applied to the skin at the receptive field focus. The impulse records in Fig. 3*A* show that the vibrotactile sensitivity of this class of thalamocortical neuron is restricted to low frequencies, reflected in the vigorous responses to the 30- and 50-Hz vibration trains but an absence of response to the 300-Hz vibration train, apart from a single onset spike.

The stimulus-response relations in Fig. 3 quantify the responsiveness of this neuron to seven frequencies of vibration by plotting the mean response as a function of vibration amplitude, and establish that maximum vibrotactile sensitivity and responsiveness occur at frequencies of ≤100 Hz where thresholds were ≤10 μm in contrast to the insensitivity at 300 Hz and relative insensitivity at 200 Hz. Maximum responsiveness (~40–60 imp/s) was apparent at 30–80 Hz when vibration amplitudes exceeded ~50 μm. Although this neuron was insensitive at 10 Hz, there were RA neurons in both the SI- and SII-projecting groups whose vibrotactile sensitivity extended down to frequencies of ≤10 Hz.

Responses of the SII-projecting RA neuron to sinusoidal vibration at 10 Hz are shown in Fig. 4*A* at amplitudes of 25, 50, and 100 μm. The neuron had a small mechanoreceptive field (~2 mm^2) on the glabrous skin of the fourth finger and was readily activated by stimulation with a 100 mg wt von Frey hair, properties that were similar to those of the SI-projecting RA neurons.

Evidence for the antidromic activation from SI and from SII, respectively, for the thalamic neurons of Figs. 3 and 4 may be seen in the collision data included in each figure. The response traces in Fig. 3, *C* and *D,* show the absence of antidromic response to SII stimulation at 3.5 mA (Fig. 3*C*) but the presence (on a background field response) of the antidromic response, at a latency of ~0.6 ms, following SI stimulation at the same strength (Fig. 3*D*). In the latter case, the cortical-evoked spike was preceded by an orthodromic spike, 2 ms beforehand, that was too early to cause collision, in contrast to circumstances in Fig. 3*E* in which the orthodromic spike shifted to within 1.7 and 1.5 ms of where the antidromic spike would have been expected.

In Fig. 4*B* the antidromic response (▽) to SII stimulation (S) occurs at a latency of 0.6 ms, in four of five superimposed traces, but in none of the traces following SI stimulation (S in Fig. 4*C*). The antidromic spike from SII is present in the two traces in Fig. 4*D* where the orthodromic spikes precede it by >3 ms but is extinguished in Fig. 4*E* when the orthodromic spikes are within ~2 ms of the expected antidromic response.

Functional capacities of SI- and SII-projecting neurons sensitive to high-frequency vibration

Both SI- and SII-projecting groups of thalamic neurons contained purely dynamically sensitive neurons that displayed a selective sensitivity to vibrotactile stimuli at high frequencies (in particular, >100 Hz) and whose properties were consistent with their peripheral input being derived from Pacinian corpuscle-like receptors (Coleman et al. 2001). As was the case for the RA class of thalamocortical neurons, there appeared to be a differential representation of this PC-related class in the SI- and SII-projecting samples (Table 1). However, the representatives of this class in the two projection groups displayed similar and consistent properties. Both SI- and SII-projecting neurons of the PC class could be activated by low strength von Frey hairs (usually <100 mg wt) from larger receptive fields than were found for RA-related neurons, and in both groups displayed very low thresholds (<5 μm) to high-frequency vibratory stimuli. Representative responses from one of the four SI-projecting PC neurons to 300-Hz vibration at 5, 30, and 50 μm are illustrated in Fig. 5*A*. The related stimulus-response

Downloaded from http://jn.physiology.org/ by 10.220.33.4 on September 27, 2016

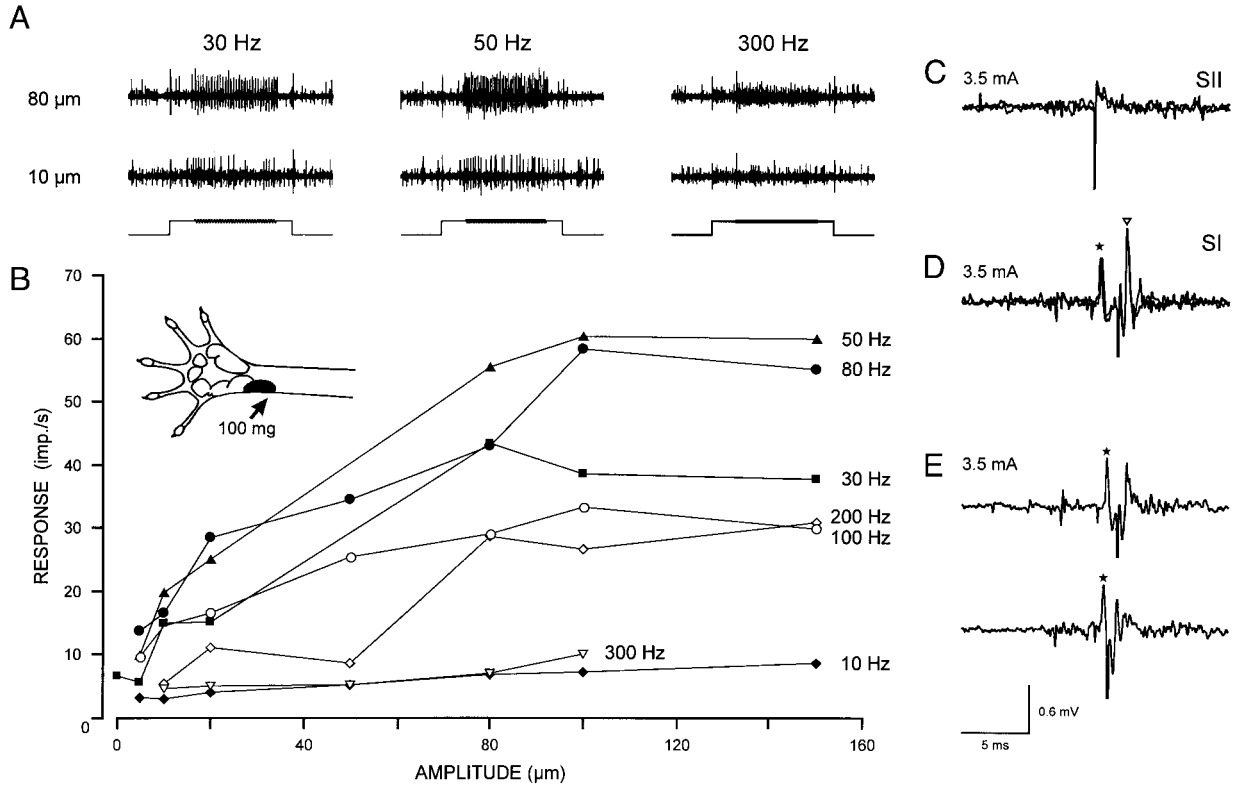

FIG. 3. Response data from a rapidly adapting (RA) thalamocortical neuron that projected to SI. Impulse traces in *A* show the responses of the neuron to vibration at 30, 50, and 300 Hz, at amplitudes of 10 and 80 μm. The stimulus waveforms show the 1-s vibration train superimposed on a 1.5-s skin indentation, applied within the receptive field of the neuron (figurine in *B, inset*). Although at 300-Hz vibration another neuron was activated (smaller spikes), the neuron activated at the 2 lower frequencies could be reliably discriminated because of its larger amplitude spikes. In *B,* responses of the neuron (imp/s $\pm$ SD, $n = 10$) are plotted for 7 frequencies (10, 30, 50, 80, 100, 200, and 300 Hz) as a function of vibration amplitude. Evidence that this thalamic neuron projected to SI is shown in *C–E.* In *C,* the neuron failed to respond to a 3.5-mA current (downward deflection in the 3 superimposed traces) applied to the SII hand area. In *D,* the neuron responded (⋆) to the peripheral mechanical tap stimulus (100 μm, 3 ms) and then (▽) to the electrical stimulus (downward deflection) applied to the SI hand area at 3.5 mA (threshold was 2 mA). As the cortical stimulus was brought closer to the peripherally evoked spikes (⋆) in the 2 traces in *E,* the cortical stimulus failed to elicit a response because of collision.

relation constructed from these and other responses of the neuron are plotted in Fig. 5*B*. The smaller graph plotted as the *inset* in Fig. 5*B* shows the profile or bandwidth of frequency sensitivity for this neuron (continuous line) and for four other SI-projecting PC neurons and was derived by plotting the mean response level at different vibration frequencies at a fixed vibration amplitude (30 μm). This relation shows the preferential responsiveness of the neuron to the high vibration frequencies and relative insensitivity below 100 Hz.

The five SII-projecting neurons of the PC-related class displayed similar vibrotactile sensitivity and bandwidths to their SI-projecting counterparts as reflected in the Fig. 6 data for a representative SII-projecting neuron of this class. The impulse traces in Fig. 6*A* and associated stimulus-response relation in Fig. 6*B* reveal the exquisite sensitivity of this neuron to the 300-Hz vibratory stimulus applied to its receptive field on the glabrous skin of the thumb. The bandwidth of vibration sensitivity, from $<$100 Hz to $>$600 Hz, is demonstrated for this neuron in the responsiveness profile plotted in the continuous line in the *inset* of Fig. 6*B* at a fixed vibration amplitude of 20 μm, together with the profile for the few other SII-projecting neurons. The collision data confirming the antidromic nature of the SI- and SII-induced responses in Figs. 5 and 6, respectively, is contained in the impulse traces of Figs. 5, *C–E,* and 6, *C–E* (see legends for details).

Capacity of SI- and SII-projecting thalamocortical neurons to signal temporal features of vibrotactile stimuli

PC afferent fibers and their central target neurons respond over the major part of the vibrotactile frequency range, from below 100 Hz to the upper limit of vibrotactile sensibility (about 1,000 Hz), and account for frequency recognition and discrimination at these high frequencies (Burton 1986; Ferrington and Rowe 1980a,b; Jänig et al. 1968; Mountcastle et al. 1969; Talbot et al. 1968).

The tightness of phase locking in the responses of SI- and SII-projecting PC neurons to vibration was examined *qualitatively* by inspection of impulse trace records (Figs. 7 and 8) and *quantitatively* by construction of phase-scatter graphs and cycle histograms from which measures of phase locking could be derived (Figs. 7–9). Although some adaptation occurred in responses over the one second period of vibration, the neurons in both projection groups responded at impulse rates of up to ~100 imp/s averaged over this 1-s duration of the vibration train. These impulse rates enabled neurons of both groups to respond on successive cycles of the vibration train at frequen-

Downloaded from http://jn.physiology.org/ by 10.220.33.4 on September 27, 2016

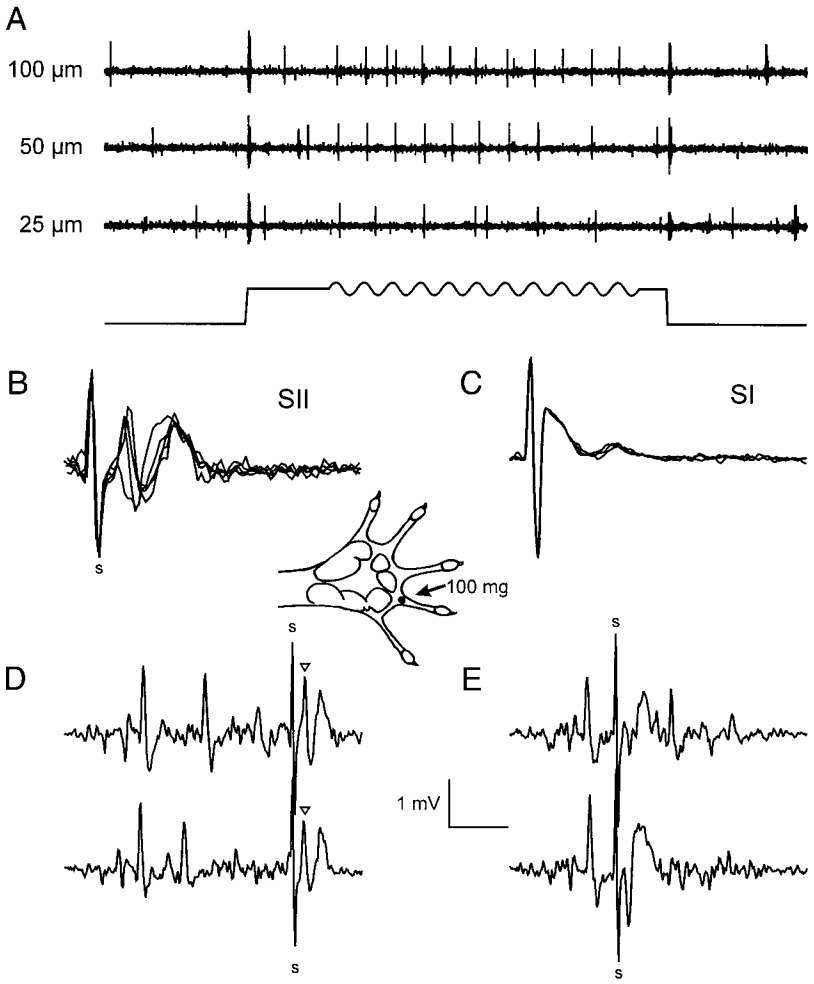

FIG. 4. Responses of an RA neuron and evidence for its projection to SII. *A*: responses to 10-Hz vibrotactile stimulation on the 4th finger (superimposed on a 1.5-s, 600-μm skin indentation; receptive field in figurine). The waveform of the mechanical stimulus is shown and vibration amplitudes indicated. In *B*, 4 of 5 superimposed traces exhibit spike responses (▽) to a 5-mA cortical stimulus (S) applied to the SII hand area. In *C*, cortical stimulation of the SI hand region did not elicit the spike response although a field potential was apparent. The onset of the traces in *D* and *E* is 4 ms delayed from the onset of a 500-μm tap stimulus applied to the neuron's receptive field. In *D*, the neuron responded to a *single* tap stimulus with a pair of spikes and to the later SII cortical stimulus (5 mA). In *E*, the SII cortical stimulus at the same strength (5 mA) could no longer elicit a spike response because of collision. The time scale is 1 ms for *B* and *C*, 3 ms for *D* and *E*. The voltage bar applies to all but *A*. The location of this RA neuron in the lateral division of the ventral posterior nucleus of the thalamus (VPL) is shown by Fig. 10.

cies of up to ~100 Hz. However, even at higher frequencies, where the limitations on discharge rate precluded a cycle-by-cycle response throughout the 1-s vibration train, the impulse activity remained phase locked to the vibration as reflected in the preferential occurrences of most spikes within a restricted phase segment of the vibration cycle waveform, indicated in Figs. 7 and 8 by the unshaded half-cycle segment of successive cycles throughout the vibration train. The response traces in Figs. 7 and 8 show that *both* the SI- and SII-projecting neurons respond to 200 and 300 Hz vibration at interspike intervals that approximate multiples of the vibration cycle period. The spike intervals in the early segments of the 1-s vibration train, shown in the *left hand block of traces* in Figs. 7 and 8, approximate 2, 3, or 4 times the cycle period, whereas in later segments (*right hand block of traces*) the interspike intervals are longer but still appear to occur on the same preferred phase of the vibration waveform.

The extent of phase locking was evaluated precisely by constructing cycle histograms and phase-scatter graphs from which quantitative measures could be derived. Those in Figs. 7 and 8 were constructed from responses at the approximate "best frequencies" (200 and 300 Hz) for the vibration-sensitive PC-related neurons and confirm that the responses of *both* SI- and SII-projecting neurons were phase locked to the vibration. The phase-scatter graphs plot, on the abscissa, the time (or phase) of impulse occurrence within the vibration cycle period (5 ms for 200 Hz and 3.3 ms for 300 Hz) against the time from the onset of the 1-s vibration train (ordinate), while the cycle histograms plot the cumulative distribution of impulse events displayed in the corresponding phase-scatter graph.

The distributions in Fig. 7 for the SI-projecting neuron reveal that impulses occur at one or other of two preferred phases of the vibration waveform, at both 200 and 300 Hz. However, at each frequency, the maximum percentage of impulses falling within any continuous half-cycle segment of the cycle histogram, a measure termed percentage entrainment (Ferrington and Rowe 1980a; Mountcastle et al. 1969; Turman et al. 1992; Zhang et al. 1996), was 98 and 87%, respectively.

For the SII-projecting neuron whose data are illustrated in Fig. 8, the percentage entrainment is even higher, with values of 100 and 97% at 200 and 300 Hz, respectively. However, a more marked decline in phase locking at higher vibration frequencies was observed for some SII-projecting neurons, as illustrated for one case in the cycle histograms of Fig. 9*A*, where percentage entrainment declined from the 98 and 95% values at 100 and 200 Hz to values of 63 and 61% at 300 and 400 Hz, respectively.

As we observed no evidence of any systematic effect of vibration amplitude on percentage entrainment (in agreement with our earlier detailed analysis of vibration-sensitive neurons in the cat somatosensory cortex) (Ferrington and Rowe 1980a), we examined the effects of vibration frequency on phase lock-

Downloaded from http://jn.physiology.org/ by 10.220.33.4 on September 27, 2016

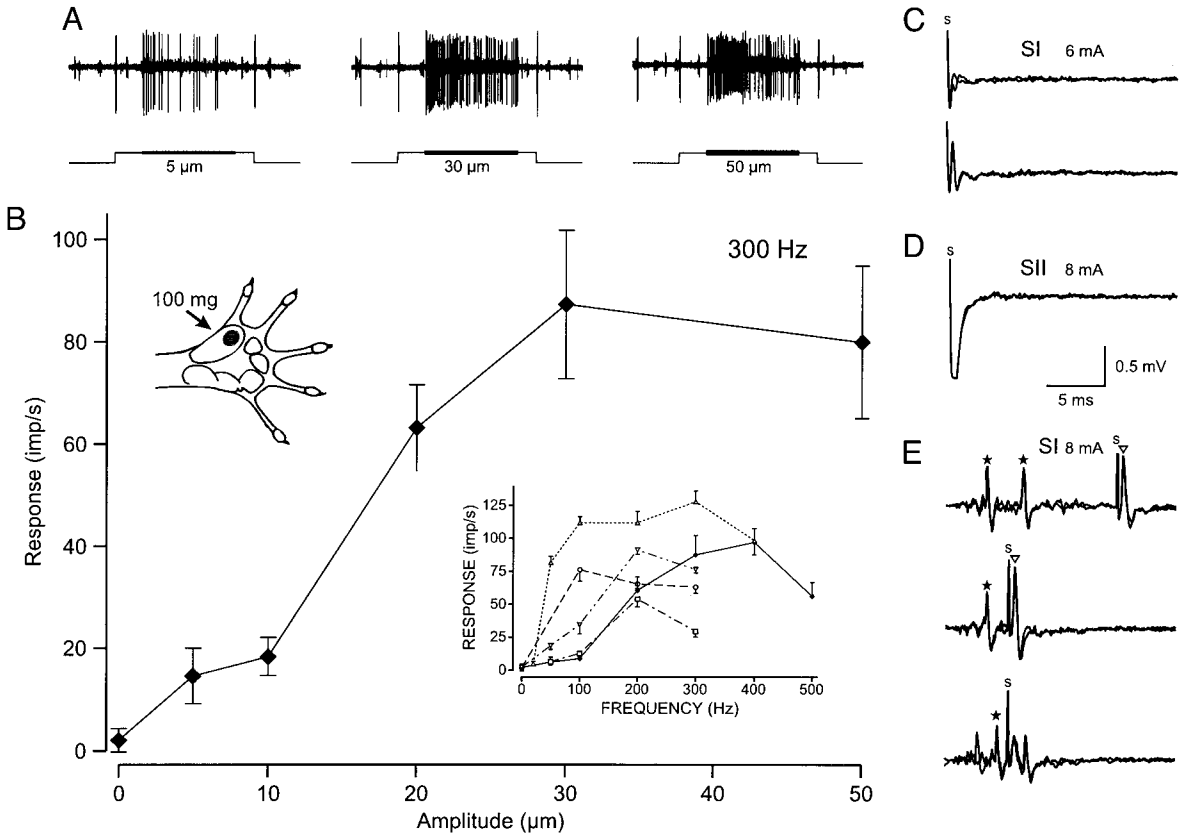

FIG. 5. Response data from a Pacinian-related thalamocortical neuron that projected to SI. This neuron had a receptive field in the thenar region (figurine in *B*) and could be activated by a <100 mg wt von Frey hair. Impulse traces in *A* show the responses to 3 amplitudes (5, 30, and 50 μm) of 300-Hz vibrotactile stimulation. Stimulus waveforms show the 1-s vibration train superimposed on a 600-μm, 1.5-s skin indentation. In *B*, the response levels to the 1-s vibration (mean ± SD in imp/s, $n = 10$) are plotted as a function of amplitude. The *inset* shows the frequency bandwidth of vibration responsiveness for this PC neuron (—), and for 4 other SI-projecting PC neurons, by plotting the mean (±SD) response level at different frequencies at a fixed amplitude of 30 μm. Evidence that the thalamic neuron of *A* projected to SI, but not to SII, is shown in *C–E*. In *C*, electrical stimulation at 6 mA (at threshold) elicited a response in ~50% of tests (response absent in *top traces*, but present in *bottom traces*). In *D*, stronger electrical stimulation at the SII focus (8 mA) failed to elicit any response in this neuron. Confirmation that the SI-induced response was antidromic was provided by the collision data in *E*. In the *top trace* in *E*, the neuron responded (⋆) to the peripheral tap stimulus, often with a doublet response (*top panel*), and then (▽) to the later SI electrical stimulus (S). In the *bottom traces*, the cortical stimulus was brought closer in time to the peripherally evoked spikes. In the *middle trace*, the 2nd peripheral spike was absent, and in the *bottom trace* the cortically induced spike was suppressed by collision from a preceding orthodromic spike (⋆). The latency of the subsequent spike (unmarked) is too long to be antidromic and appears to be the 2nd of a peripherally induced doublet response. The spike height for this neuron (in *A* and *C–E*) fluctuated somewhat with cardiorespiratory-related movement of the brain.

ing using amplitudes that generated a response level at or near the plateau response rate for the neuron, and, for a given thalamocortical neuron, held the amplitude fixed at the different vibration frequencies studied.

Quantitative comparison of phase locking for the SI- and SII-projecting samples of thalamic PC-related neurons in Fig. 9, based on plots of percentage entrainment as a function of vibration frequency, reveals considerable variability from neuron-to-neuron within each sample. The mean values for the five SI-projecting neurons (plotted in Fig. 9*B*) are compared in Table 2 with those for the four SII-projecting neurons (from Fig. 9*C*). The two samples overlap in these measures, with almost identical mean values at 200 and 300 Hz, and perhaps marginally higher values for the SII-projecting neurons at other frequencies. However, with the small samples on which these detailed measures can be obtained, it is not possible to conclude or infer that there is any systematic difference between the samples. Instead, the conclusion must be that the information about vibration frequency conveyed directly to SII over this class of projecting neurons *at least* matches that conveyed directly to SI. Furthermore, the properties of both SI- and SII-projecting groups of PC-related thalamocortical neurons in the marmoset appear similar to those identified for thalamocortical neurons of this class in the cat (Ghosh et al. 1992).

Locations of SI- and SII-projecting neurons in the thalamus

The 44 thalamic neurons shown to project to SI were located at depths of 7.0–11.1 mm below the surface of the overlying parietal cortex, while the 11 SII-projecting neurons were recorded at depths between 7.9 and 11.9 mm. As might be expected from the similar range of depths, covering approximately 4 mm for both samples, there was no difference statistically ($P = 0.1$) between the mean depths for the groups. Furthermore, in *individual* experiments there was no evidence for a differential grouping of SI- and SII-projecting neurons,

Downloaded from http://jn.physiology.org/ by 10.220.33.4 on September 27, 2016

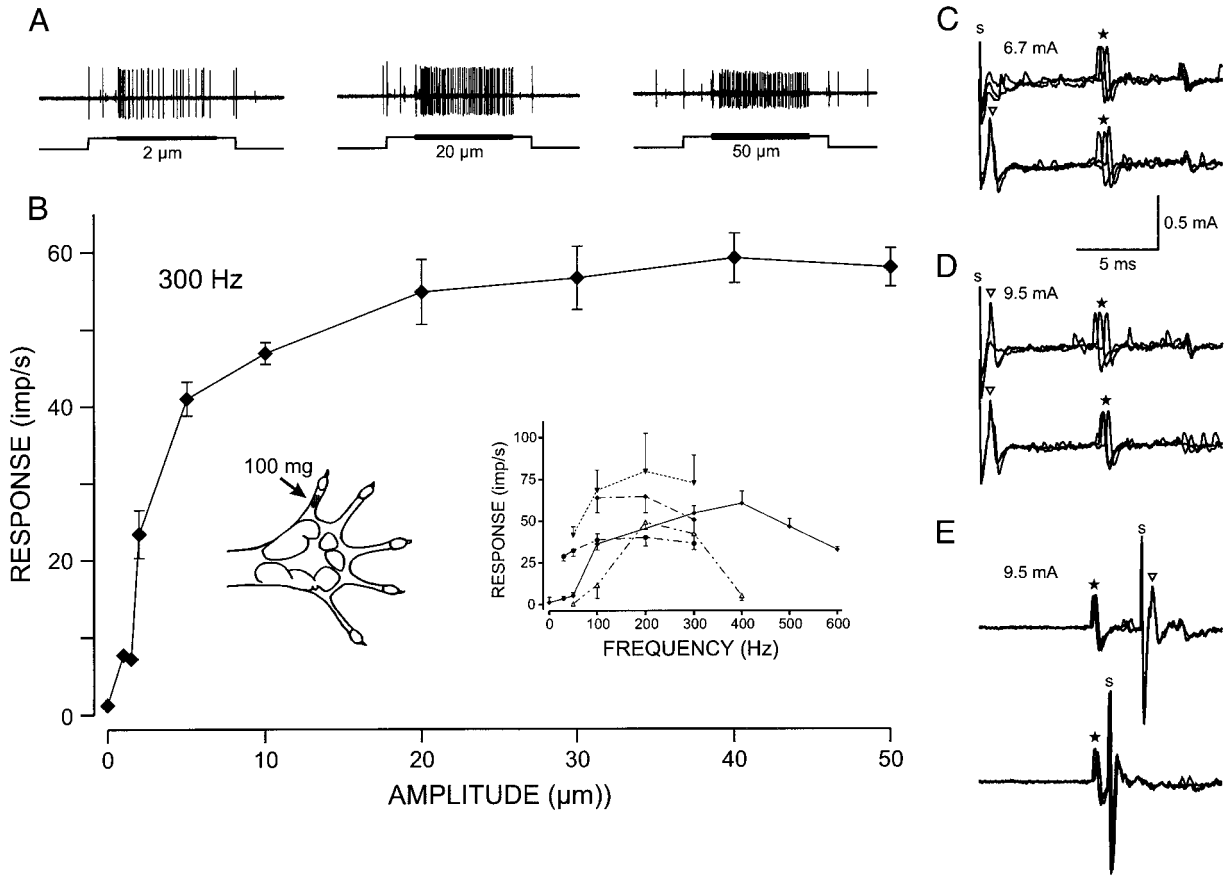

FIG. 6. Response data from a Pacinian-related thalamocortical neuron that projected to SII and could be activated by a 20 mg wt von Frey hair from the thumb (receptive field in figurine). Impulse traces in *A* show the responses to 3 amplitudes (2, 20, and 50 μm) of a 1-s long 300-Hz vibrotactile stimulus superimposed on a 400-μm, 1.5-s skin indentation. In *B*, the response levels (mean ± SD in imp/s, $n = 10$) are plotted as a function of vibration amplitude. The *inset* in *B* shows the bandwidth of vibratory responsiveness for this neuron (—) and for 4 other SII-projecting PC neurons. Each point in the *inset* represents the mean (±SD) response level at different vibration frequencies at a fixed amplitude of 20 μm. Evidence that this thalamic neuron projected to SII is shown in *C–E*. Each consists of 3 superimposed traces, showing peripheral-evoked responses at a latency of ~7.5 ms (⋆) from a 3-ms, 100-μm tap stimulus, and cortically evoked activation (▽) of the neuron. In *C*, a near-threshold SII stimulus (S; 6.7 mA, 50 μs) elicited responses from this neuron in some cases (*bottom traces*) but not others (*top traces*). In *D*, the higher strength SII stimulus (9.5 mA) elicited responses in almost every trial. In *E, top trace*, the neuron responded first (⋆) to the peripheral tap stimulus and then (▽) to the later SII electrical stimulus (S, 9.5 mA). As the cortical stimulus was brought closer to the peripherally evoked spikes in the *bottom trace* in *E*, the cortical stimulus failed to elicit a response, demonstrating that the neuron projected to SI.

for example, with SII-projecting neurons located ventral to the SI-related neurons. This might have been predicted if the traditionally designated ventral posterior inferior (VPI) subnucleus (Jones 1985) were the source of SII-projecting neurons as has been suggested by Friedman and Murray (1986) (however, see DISCUSSION). In the histological reconstructions of electrode tracks through the VP nucleus in Fig. 10*A*, an SII-projecting neuron (△) was found above two SI-projecting neurons (◆) in the *right hand track* (the neuron marked by the cross in the *left hand track* was a nonprojecting neuron). Furthermore, the nine electrode tracks in which two or more projection neurons were identified and which have been reconstructed in Fig. 10*B* according to medio-lateral position, show that SII-projecting neurons (△, ○, and ◇) were encountered both above and below SI-projecting neurons (filled symbols).

We also found no evidence of differential groupings of the thalamocortical neurons according to their functional class. In Fig. 10 the PC-related thalamocortical neurons, whether projecting to SI (▲) or to SII (△) were found above RA and SA-related classes in several tracks (Fig. 10, *A* and *B*, and Fig. 11) and below these classes in other tracks (Fig. 10*B*). In Fig. 11, for example, the reconstructed electrode track through the VPL nucleus shows, in close proximity, the locations of three identified SII-projecting neurons that were of different functional classes. The first, at a depth of 8.0 mm, responded to just the dynamic components of a step indentation delivered to its receptive field on the palm and was selectively sensitive to high-frequency vibration. Its peripheral tactile input therefore appeared to be derived selectively from Pacinian corpuscle receptors. The second, 0.3 mm deeper, also displayed a pure dynamic mechanosensitivity but was selectively sensitive to low-frequency vibratory stimulation on the glabrous skin of the fourth finger, indicative of an RA afferent source of input. Deeper still, at 8.5 mm below the cortical surface, was a slowly adapting tactile neuron activated by static displacement of the glabrous skin of the fifth finger. These histological reconstructions demonstrate clearly that there is no systematic segregation in dorsoventral location in the mar-

Downloaded from http://jn.physiology.org/ by 10.220.33.4 on September 27, 2016

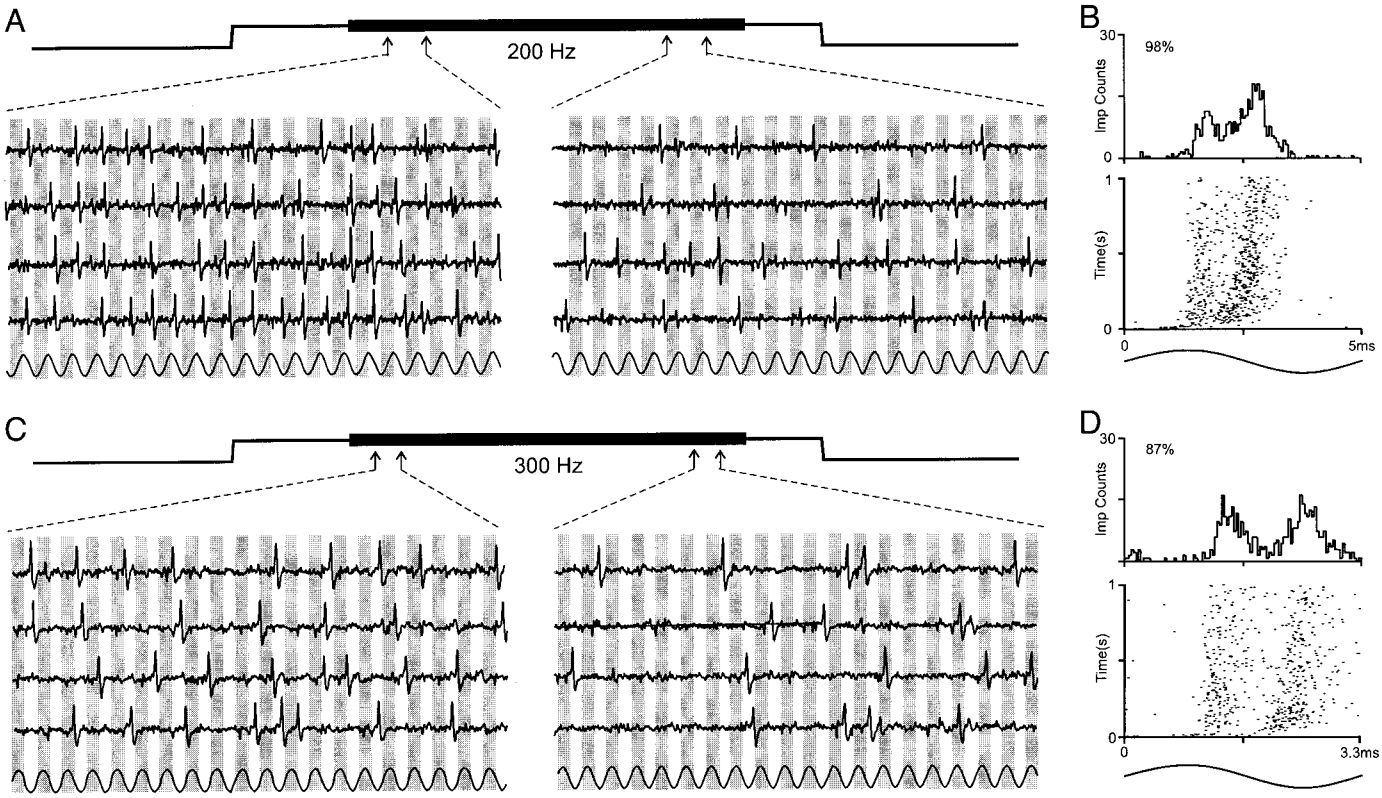

FIG. 7. The pattern of impulse activity in responses of an SI-projecting PC neuron to vibrotactile stimuli at 200 Hz in *A* and *B* and 300 Hz in *C* and *D*. Five sets of impulse trains in response to 20 vibration cycles near the beginning and end of the 1-s vibration (at the times indicated) are displayed on the *left* and *right panels*, respectively. The shaded strips represent ½ the duration of each sine-wave cycle and have been aligned to emphasize the phase locking of responses, with most impulses falling in the nonshaded half-cycle segments. The actual phase relation between impulse activity and the vibration waveform is not known because of conduction and synaptic delays. The phase scatter graphs in the *bottom part* of *B* and *D* plot the time of each impulse occurrence (single dot) during each cycle period (abscissa) as a function of time after the onset of the 1-s vibration train (ordinate). Cycle histograms in the *top parts* of *B* and *D* share the same abscissa as the phase scatter graphs and display the cumulative distribution of impulse occurrences within the vibration stimulus cycle. Despite the occurrence of impulses at 2 preferred segments of the vibration cycle, this SI-projecting thalamic neuron had a tightly phase-locked response, as shown by the peaks in the cycle histograms in the *top part* of *B* and *D*, as well as by the high percentage entrainment values (98% for 200 Hz and 87% for 300 Hz).

moset VPL according to either functional class, as has been suggested for the VPL nucleus in the squirrel monkey (Dykes et al. 1981), or according to the cortical projection target of the thalamic neuron.

DISCUSSION

Thalamocortical tactile systems in the marmoset: background to a controversy

The organization of thalamocortical tactile systems in primates has been a matter of controversy since reports emerged that the SI and SII areas of cortex were arranged in a serial, or hierarchically organized scheme in which tactile information is conveyed from the thalamus to SI, and thence to SII as the next hierarchical level of processing (Garraghty et al. 1990b; Pons et al. 1987, 1992). This serial processing hypothesis was based on experiments in which SII responsiveness disappeared in both macaque and marmoset monkeys following surgical ablation of SI and was proposed despite known anatomical projections from the thalamus to *both* the SI and SII areas (for reviews see Burton 1986; Jones 1985; Steriade et al. 1997). Furthermore, this serial organizational scheme proposed for primates proved to be very different from the functional arrangement identified in a variety of nonprimate mammals in which SI and SII were found to be organized in parallel (see INTRODUCTION).

The issue became more controversial with our re-investigation of the serial/parallel processing issue for SI and SII in the marmoset monkey with localized cortical cooling for SI inactivation, which demonstrated, in contrast to the earlier ablation study, a very substantial, perhaps exclusive parallel organization of SI and SII for tactile processing (see INTRODUCTION) (see also Zhang et al. 1996). Although a proportion of SII neurons showed some reduction in responsiveness in association with the SI inactivation, there were several lines of evidence that this was attributable to the loss of a background facilitatory influence operating from SI. In the present study and the companion paper (Zhang et al. 2001), we have used two different approaches to clarify the thalamocortical organizational scheme that operates for SI and SII in the marmoset monkey. The approach reported in Zhang et al. (2001) was based on an analysis of SI responsiveness in association with reversible inactivation of SII to determine whether the two areas occupy hierarchically equivalent positions in a parallel,

Downloaded from http://jn.physiology.org/ by 10.220.33.4 on September 27, 2016

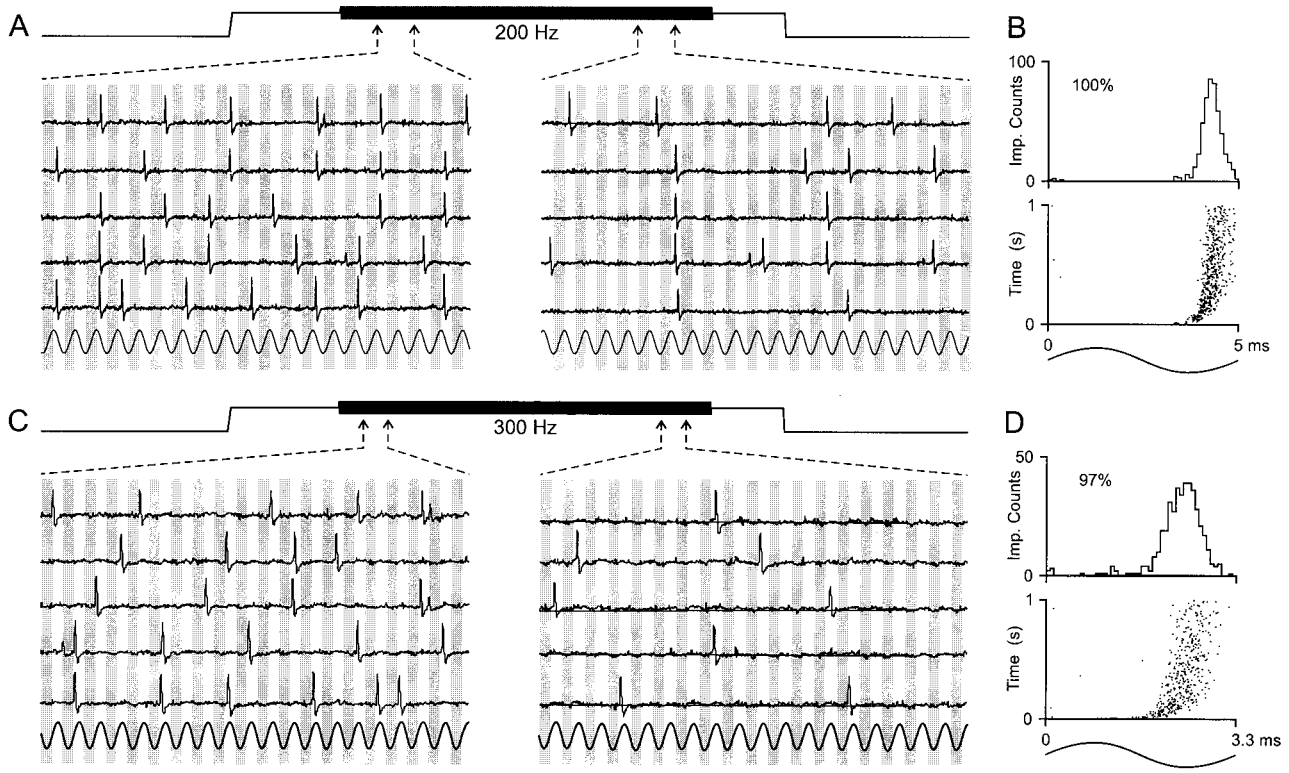

FIG. 8. Patterns of impulse activity of an SII-projecting PC neuron in response to vibrotactile stimuli at 200 Hz in *A* and *B* and 300 Hz in *C* and *D*. Format as in Fig. 7. Five sets of impulse trains in response to 20 cycles near the beginning and end of the 1-s vibration are displayed in the *left* and *right panels* of *A* and *B*, respectively. The tight clustering of impulse occurrences in the phase scatter graphs and cycle histograms in *B* and *D*, and the high percentage entrainment values (100% for 200 Hz and 97% for 300 Hz), demonstrate that the responses of this SII-projecting thalamic neuron were very tightly phase locked to the vibration stimulus.

distributed processing scheme. In contrast, the approach in the present paper was to examine the functional properties of the thalamic neurons that provide the input to SI and SII, to determine whether the *direct* thalamic input can account for the tactile processing that takes place in these two cortical areas.

Functional identification of SI- and SII-projecting neurons of the ventral posterior thalamic nucleus

The present demonstration that low-threshold tactile inputs are conveyed directly from the thalamus to SII as well as to SI depended on identification of the thalamic neurons in terms of their cortical projection target, a requirement that was met by antidromic identification of the neurons from the SI- or SII-projection focus for the hand. Activation of the thalamic neuron from the cortex is not enough to establish a cortical projection as this could take place by transynaptic activation, either via cortico-thalamic descending systems or as a consequence of antidromic activation of other thalamocortical neurons whose collateral axonal connections within the thalamus may lead to activation of the recorded neuron. The only neurons that we accepted therefore as having a genuine axon projection to SI or SII were those for which there was evidence for collision and extinction of the cortically generated spike, by a prior peripherally generated spike, over a time period in excess of twice the latency for the cortically generated response (see METHODS).

This collision technique for verification of the antidromic nature of the response is illustrated in Figs. 1–6 and provides the most reliable functional identification of the SI- or SII-projecting thalamocortical neuron (see METHODS) (and see Darian-Smith et al. 1963; Fuller and Schlag 1976). With this technique we confirmed a cortical projection to SI or SII for 55 thalamic VP neurons. Although the majority projected to SI, the proportions probably reflect the substantially larger area of the hand and forelimb representation in SI compared with SII in the marmoset (see *Location of SI- and SII-projecting neurons in the thalamic ventral posterior nucleus*) (and see Zhang 1994; Zhang et al. 1996) and therefore the incidence of SI- and SII- projecting neurons within the thalamic VP nucleus.

Representation of different functional classes among SI- and SII-projecting thalamic VP neurons

The sample size, in particular, for the SII-projecting neurons, is too small to permit precise conclusions about the proportions of the different functional classes of tactile neurons that project to SI compared with SII. However, from these limited samples it appears that projection ratios may be different. For example, among the small SII-projecting sample, the ratios for different functional classes associated with the hand were approximately 20–30% SA, 10% RA, 50% PC, and 10–20% deep input, whereas among SI-projecting neurons it was ~10% SA, 60% RA, 10% PC, 20% HFA or deep-related neurons. Neither sample reflected closely the proportions of the three major tactile classes identified in the associated study of

Downloaded from http://jn.physiology.org/ by 10.220.33.4 on September 27, 2016

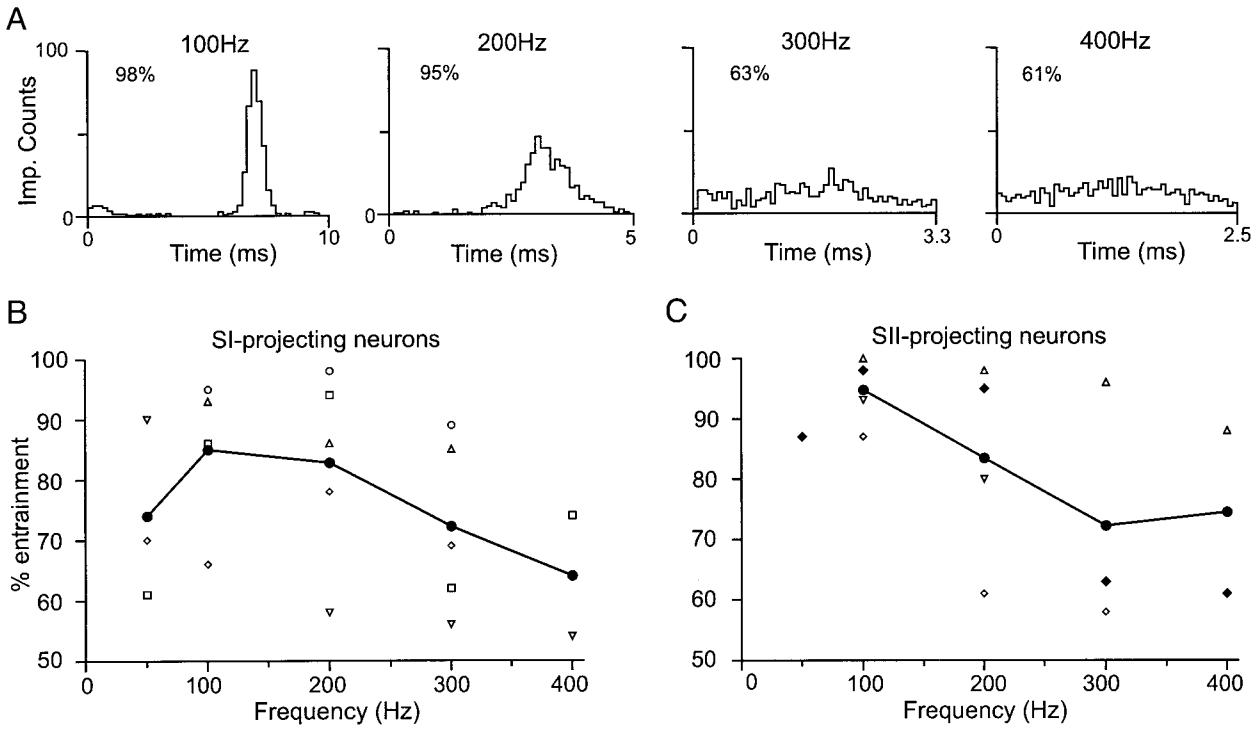

FIG. 9. Phase locking in vibration-induced responses of SI- and SII-projecting thalamocortical neurons. *A*: cycle histograms (CHs) constructed from responses of an SI-projecting neuron that appeared to receive inputs predominantly from Pacinian sources. Each CH was constructed from responses to 10 repetitions of the vibration train at the frequencies indicated and a fixed 30-μm amplitude. (Stimulus-response relations and collision data are plotted for the same neuron in Fig. 5.) Percentage entrainment as a function of vibration frequency is plotted for the 5 SI-projecting neurons (*B*) and for 4 SII-projecting neurons (*C*). Continuous lines connect mean values that were derived from the individual values plotted at each frequency.

primary afferent fibers innervating the marmoset hand (Coleman et al. 2001) where we found 55% of fibers of the SA class, 32% RA, and 13% PC. However, earlier data on the representation of different functional classes of tactile neurons associated with the distal limb have also shown marked variation, whether at the afferent fiber, cuneate, or thalamic levels (Douglas et al. 1978; Ghosh et al. 1992; Lindblom 1965; Pubols and Pubols 1973, 1976; Talbot et al. 1968) or within the cortex. For example, in the cat SII area, ratios of ~1:13:6 were found for SA, RA, and PC-related neurons (Bennett et al. 1980), and in the macaque SI area, the ratio was ~3:16:1 (Mountcastle et al. 1969). However, the significance of these different ratios is uncertain and needs to be viewed with caution as data come from different species, from different laboratories, and in the presence of different anesthetic regimens.

TABLE 2. *Measures of phase locking in vibration-induced responses of PC-related VP thalamic neurons projecting to SI and SII*

	Percentage Entrainment	
Vibration Frequency	SI-projecting	SII-projecting
50 Hz	71 (4)	94 (2)
100 Hz	85 (5)	95 (4)
200 Hz	83 (5)	84 (4)
300 Hz	72 (5)	72 (4)
400 Hz	64 (2)	75 (2)

Values are mean percentage entrainment for the number of neurons indicated in parentheses. VP, ventral posterior; for other abbreviations, see Table 1.

Nevertheless, the points that may be emphasized from the present analysis of SI- and SII-projecting VP thalamic neurons are first, that the major classes of tactile afferent input from the glabrous surface of the hand were identified in the projection to *both* cortical targets. These included neurons activated by static tactile stimuli, whose input comes from the SA class of afferent fiber innervating the hand, and purely dynamically sensitive neurons (Coleman et al. 2001) that could be subdivided into two broad classes. One of these appeared to be activated by Pacinian-related sources and the other by the presumed intradermal class of dynamically sensitive tactile receptors associated with afferent fibers that, in different studies, are identified as RA (Ferrington and Rowe 1980b; Iggo and Ogawa 1977; Jänig et al. 1968) QA (Johnson 1974; Talbot et al. 1968), or fast adapting type I (FAI) fibers (Johansson and Vallbo 1983). This dichotomy among the dynamically sensitive thalamocortical projection neurons appears to correspond well with the two broad groups of dynamically sensitive tactile fibers that were identified in association with the glabrous skin of the marmoset hand in our related study (Coleman et al. 2001).

The substantially higher proportion of RA neurons represented among the SI-projecting neurons (Table 1) may imply a major role for SI in the processing of low-frequency vibrotactile information, whereas the higher incidence of PC repr esentation among the SII-projecting neurons (Table 1) may support the hypothesis of a differential role for SII in high-

Downloaded from http://jn.physiology.org/ by 10.220.33.4 on September 27, 2016

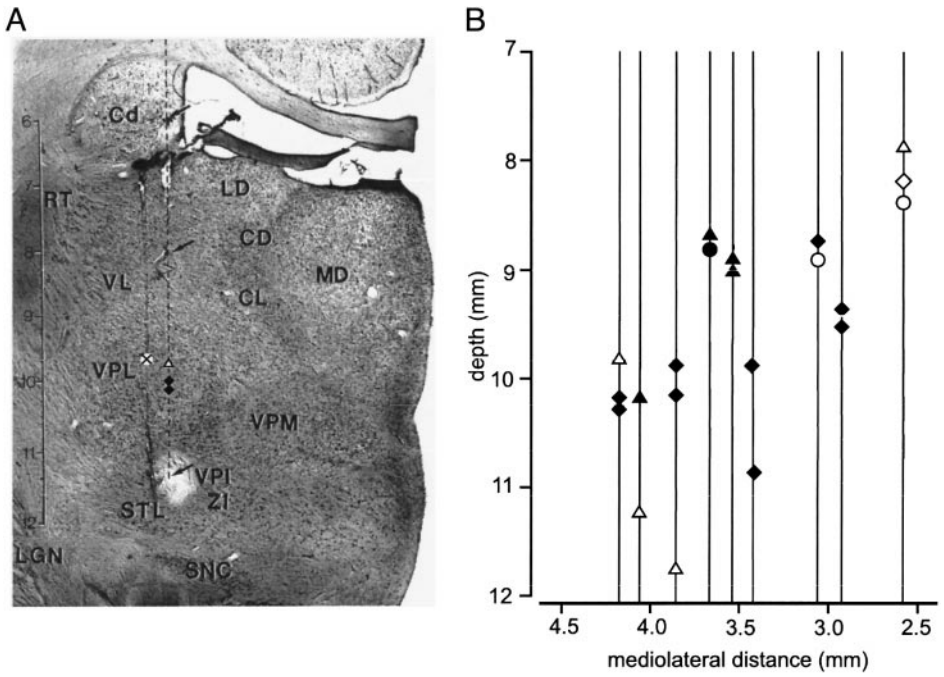

FIG. 10. Histological reconstructions of electrode tracks through the marmoset ventral posterior (VP) nucleus. *A*: a coronal section (anterior view of the right hand side) with the location of 2 electrode tracks in which a nonprojecting neuron was recorded (*left hand track*) and 3 projecting neurons were studied (*right hand track*). The 3 neurons were, respectively, according to depth, an SII-projecting PC neuron, and 2 SI-projecting RA neurons. The 3 arrows indicate the location of lesions made by passing current (see METHODS) through the electrode at the end of the experiment. Labels indicate the following nuclei: Cd, caudate; CD, central-dorsal; CL, central-lateral; LD, laterodorsal; LGN, lateral geniculate; MD, mediodorsal; RT, thalamic reticular; SNC, substantia nigra compacta; STL, subthalamic Luysi; VL, ventrolateral; ZI, zona incerta. *B*: 9 electrode tracks, in which 2 or more thalamocortical projection neurons were isolated, have been reconstructed from different experiments according to their mediolateral position. The depth locations of SI- and SII-projecting neurons (filled and open symbols, respectively) of different functional classes are indicated by triangles (PC neurons), diamonds (RA neurons), and circles (SA neurons).

frequency vibrotactile processing (Ferrington and Rowe 1980a; Fisher et al. 1983; Rowe et al. 1985).

Comparison of functional properties of SI- and SII-projecting thalamic VP neurons

The *second* point to be emphasized from the present study is that, within a given neuron class identified in the projection to SI and SII, there appeared to be no systematic distinction in functional properties between those projecting to SI and those projecting to SII. There was therefore no distinction at this level that might be consistent with thalamic inputs to SI having the capacity to *activate* SI target neurons while thalamic inputs to SII should be "*nonactivating*" as has been proposed on the basis of SII responsiveness being abolished by surgical ablation of SI (Garraghty et al. 1990a,b). The SI- and SII-projecting neurons of the *SA* class appeared indistinguishable in functional properties, based on the similar form of their stimulus-response relations (Figs. 1 and 2), their von Frey thresholds for activation and receptive field characteristics, and their overlap on a number of quantitative measures derived from the stimulus-response relations. These included their thresholds to static displacement, the slope of the relations, and the maximum impulse rates generated by static skin displacement. Although disparate proportions of SI- and SII-projecting neurons of the RA class were found, the SII-projecting neuron of Fig. 4, with its vibration sensitivity confined to low frequen-

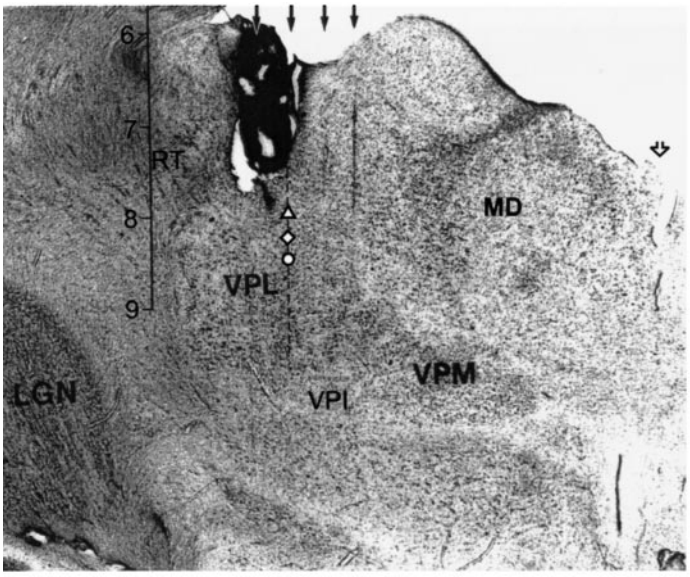

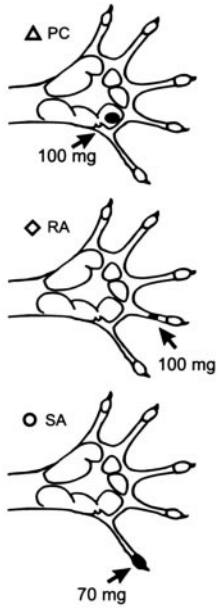

FIG. 11. Location of an electrode track (dashed line) in which 3 SII-projecting neurons were identified at depths below the cortical surface of 7.9, 8.3, and 8.5 mm, respectively, within the VPL thalamus (anterior view of the right side). Four electrode penetrations (separation 300 μm) were made at this coronal plane as indicated by the solid arrows. These 3 neurons, whose receptive fields are indicated in the figurines on the *right hand side*, belonged to different functional classes and were, respectively, in depth, related to PC, RA, and SA sources. Response records for one of them, the RA neuron, are shown in Fig. 4. The hematoma at the dorsolateral corner of the thalamus was caused by a marker electrode left at the end of experiment. The open arrow indicates the midline. LGN, lateral geniculate nucleus; RT, thalamic reticular nucleus; MD, mediodorsal nucleus. Nissl stain, 75 μm in thickness.

Downloaded from http://jn.physiology.org/ by 10.220.33.4 on September 27, 2016

cies, fell within the range of functional properties of RA neurons in the larger SI-projecting sample.

More detailed comparative analysis of the SI- and SII-projecting neurons of the PC-related class revealed a consistency of properties that permit the confident conclusion that low-threshold, high acuity tactile information is conveyed to *both* SI and SII about the dynamic skin perturbations that predominantly recruit the PC class of afferent fibers. The use of controlled, high-frequency sinusoidal vibration to quantitatively evaluate the capacities of thalamic neurons processing this class of input showed that both SI- and SII-projecting groups were activated at low thresholds (<5 μm at high vibration frequencies such as 300 Hz) and were sensitive across a broad bandwidth of vibration frequencies (from <100 Hz to $\sim$500 Hz). Furthermore, both groups responded with similar, tightly phase-locked activity at vibration frequencies up to 200–300 Hz and showed declining phase locking above 300 Hz (Figs. 7–9).

For both projection groups it appeared that the concatenation of functional properties was consistent with a capacity to contribute to vibration frequency recognition and discrimination. This capacity appears to depend on the temporal precision of impulse patterning in the responses to the vibratory stimuli, a coding task [as one may infer from psychophysical data, e.g., Goff (1967) and Rothenberg et al. (1977), revealing a marked increase above 200 Hz in the *Weber Fraction* ($\Delta f/f$) for vibrotactile frequency discrimination] that becomes more difficult as the vibration cycle period diminishes (with increasing vibration frequency) toward the duration of the signaling event itself, the individual action potential. Because of these demands on temporal coding, the responses of the PC-class of thalamocortical neurons to high-frequency vibrotactile stimuli provide a sensitive indicator of the similarity of SI- and SII-projecting neurons in their capacity to encode these temporal features of vibrotactile stimuli.

The low incidence of HFA input to SI (2 projection neurons; Table 1) and the apparent absence of HFA projection to SII simply reflects our concentration on tactile inputs from the glabrous skin of the hand. However, we know from our previous study of marmoset SII neurons (Zhang et al. 1996) in which $\sim$20% of the sample were activated by HFA inputs, that tactile responsiveness was retained in all but one SII neuron of this class during SI inactivation. Thus we may infer that, in the marmoset, the HFA class of input gains direct access to SII from the thalamus along with the SA, RA, and PC-related classes discussed above. The properties of all these classes and, in particular, the similarity of functional properties of the SI- and SII-projecting neurons of a given class appear to be entirely consistent with an afferent path through the dorsal column nuclei to these thalamic neurons (Brown et al. 1974; Douglas et al. 1978; Dykes et al. 1982). The data therefore provide little support for the hypothesis that the major or only thalamic source of input for SII is derived from the spinothalamic tract with inputs providing information about tactile stimuli that extends into the painful range (Krubitzer and Kaas 1992). The latter view has been linked to the hypothesis that the input to SII comes selectively from the thalamic VPI subnucleus (Friedman and Murray 1986; Garraghty et al. 1991; Krubitzer and Kaas 1992).

Comparison of functional properties of thalamocortical tactile neurons in the marmoset with those of other species

Although there have been many electrophysiological studies of tactile neurons in the thalamic ventral posterior region in different species, most studies have concentrated on the pattern of body representation or have relied largely on qualitative observations on the neurons (e.g., Dykes et al. 1988; Kaas et al. 1984; Loe et al. 1977). However, comparisons with the cat can be made for the three classes of marmoset thalamocortical neurons driven by glabrous skin tactile inputs. In both species the SA neurons show graded stimulus-response relations as a function of static skin indentation, although the dynamic range of indentation leading to a plateau in response level appears to be broader (1–2 mm) for the cat (Ghosh et al. 1992; Golovchinsky et al. 1981) than for the marmoset SA neurons (0.5–1 mm; Figs. 1 and 2).

In the dynamically sensitive classes, the RA neurons in the cat and marmoset appear similar as both display vibrotactile thresholds as low as 5–15 μm at their best frequencies of 30–80 Hz and a marked decline in vibrotactile responsiveness at vibration frequencies >100 Hz. Furthermore, PC-related neurons in the two species were similar, in displaying very low thresholds (<2–5 μm) and abrupt increases in their stimulus-response functions at their optimal vibrotactile frequencies of 200–300 Hz (Fig. 1 in Ghosh et al. 1992) (and Figs. 5 and 6, present paper). They also show similar broad bandwidths of vibration sensitivity (from <100 Hz to >500 Hz) and retain phase-locked responses to vibration up to $\sim$400 Hz (Fig. 5, Ghosh et al. 1992) (and Figs. 8 and 9, this paper).

Location of SI- and SII-projecting neurons in the thalamic ventral posterior nucleus

There was no evidence of a segregation of the identified SI- and SII-projecting thalamic neurons within different regions of the VP nucleus. Furthermore, statistical comparison of the depth distributions for these two projection groups confirmed the absence of any difference in their distributions in this dimension and rules out the possibility that the SII-projecting neurons are selectively grouped in a traditionally defined (Jones 1985), ventrally located VPI subnucleus. The results are therefore consistent with the many previous reports that SII-projecting neurons arise in the main VPL nucleus in both the macaque monkey and the cat (e.g., Burton 1984; Burton and Jones 1976; Burton and Kopf 1984; Burton and Robinson 1981; Fisher et al. 1983; Jones and Powell 1970; Macchi et al. 1959; see reviews by Burton 1986; Jones 1985), rather than being confined to an inferior location in the VPI subnucleus.

Although the border between VPL and VPI has always been somewhat contentious, even in the macaque and the cat (Jones 1985; and see discussions in Turman et al. 1992; Zhang et al. 1996), it has become more contentious in the case of the marmoset, where it has been proposed that the VPI nucleus is not confined to a location inferior to VPL but, instead, forms a fragmented entity with fingerlike extensions scattered through and around VPL including its *dorsal* as well as inferior margins (Krubitzer and Kaas 1992). The definition of these patchy, discontinuous zones as VPI has been based on these areas being the source of SII-projecting neurons and the locations of less dense cytochrome oxidase staining.

Downloaded from http://jn.physiology.org/ by 10.220.33.4 on September 27, 2016

While our findings of SII-projecting neurons being widely distributed in VP is essentially compatible with the Krubitzer and Kaas (1992) findings, our failure to observe any segregation of the two projection groups, and our observation of SI- and SII-projecting neurons in very close proximity (Fig. 10), lead us to question their redefinition of VPI where this entails a discontinuity and fragmentation of VPI almost to a single neuron level of resolution within the overall VP nucleus. We also question the redefinition as it entails an inevitable misnomer where fragments of the redefined VPI nucleus actually occupy *dorsal* locations in the overall VP nucleus. We should also emphasize that our present observations are consistent with earlier reports that there was no evidence for discrete modality or class segregation in the VP of cat (Golovchinsky et al. 1981) or macaque monkey (Chung et al. 1986), and with a recent study of body representation in the marmoset ventral posterior nucleus, which concluded that the low-threshold cutaneous receptive fields of the marmoset are organized in a "single continuous representation of the contralateral body surface" (Wilson et al. 1999).

The controversy over the thalamic VP projections to SII is perhaps compounded by the report for the macaque that there was a 94% reduction in non-GABA containing VPL neurons (together with a 54% reduction in VPL GABA-containing interneurons) following ablation of areas 3a, 3b, 1, and 2 of the SI hand representation (Chmielowska and Pons 1995). This level of degeneration appears to be a little more than might be expected from the numerous previous reports of SII-projecting neurons within VPL in both the macaque and the cat (see references above; and for review, Burton 1986; Jones 1985; Jones and Powell 1973; Steriade et al. 1997). However, a relatively low incidence of SII-projecting cells in VPL is not altogether surprising as indicated in the review by Burton (1986). He emphasized that the cortical area allocated to SII is only 10–30% of that for SI, and, as a consequence, equal areas of SI and SII covered by a given volume of retrograde tracer (or a lesion) represent very different extents of the overall topographic map in each region. Thus the SII injection covers a relatively greater proportion of the body surface representation, and one should therefore expect the retrogradely labeled SII-projecting cells to be rather scattered in VPL in comparison with a more compressed, clustered grouping of SI-projecting cells (Burton 1986). With presumably far fewer VPL neurons projecting to the smaller SII area than to SI, the lower percentage of antidromically identified SII-projecting, compared with SI-projecting neurons in the present study is therefore not surprising and is in excellent agreement with the earlier estimates by Burton (1986) that only 10–30% of the thalamic VP output goes to SII, with the remainder going to SI.

Organization of the SI and SII areas: concluding comments

The present study demonstrates directly that the major classes of forelimb-associated tactile neurons in the VPL project directly to SII as well as to SI and that individual SII-projecting neurons share the same capacity as SI-projecting neurons for signaling low-threshold, high-acuity tactile information. The results therefore confirm the existence of a parallel functional projection to SI and SII in this new-world primate species and are consistent with our other findings in the marmoset, first, that tactile responsiveness in SII largely survives the reversible inactivation of SI by cooling (Zhang et al. 1996) and, second, that SI responsiveness is largely independent of SII, and that SI and SII therefore occupy an hierarchically equivalent position in a distributed, parallel thalamocortical network for tactile processing (Zhang et al. 2001). It must therefore be concluded that there is no longer justification for the conclusion that in monkeys SII is "only distantly related to the thalamus" and "is primarily involved in processing information from other cortical fields" (Garraghty et al. 1990b).

As we have suggested before (Zhang et al. 1996), the concept that SI occupies an earlier stage than SII in a serial or hierarchical processing scheme in the marmoset (Garraghty et al. 1990b) may have arisen as an unintended consequence of the SI ablation procedure used in these earlier experiments. The ablation may have given rise to an injury discharge in the corticocortical projection to SII, leading to K^+ ion accumulation and accommodation block of the SII neurons (see INTRODUCTION). In our studies of SI-SII organization in the marmoset (Zhang et al. 1996, 2001), we have been fortunate to avoid this possible complication with the use of the reversible, cooling-induced procedure for SI or SII inactivation and have been able to quantitatively examine the responsiveness of individual neurons in each of these areas *before*, *during*, and *after* the reversible inactivation of the other area.

As we have indicated in the accompanying paper (Zhang et al. 2001), it may be appropriate to reinvestigate the claim for serial organization of SI and SII in the macaque (Pons et al. 1987, 1992) with a reversible procedure for SI inactivation in view of first, our accumulated findings for parallel organization for SI and SII in the marmoset (present paper and Zhang et al. 1996, 2001), and second, recent evidence emerging for parallel organization for SI and SII in both the owl monkey (Nicolelis et al. 1998) and in human subjects (Karhu and Tesche 1999) as discussed in Zhang et al. (2001).

We acknowledge the technical assistance of C. Riordan and D. Sarno. We are grateful to Dr. Margaret Rose for accommodation and veterinary care of the marmosets.

This work was supported by the Australian Research Council and by the National Health and Medical Research Council of Australia.

Present address of H. Q. Zhang and S. P. Zhang: School of Chinese Medicine, Hong Kong Baptist University, Hong Kong.

REFERENCES

ALLOWAY KD, SINCLAIR RJ, AND BURTON H. Responses of neurons in somatosensory cortical area II of cats to high-frequency vibratory stimuli during iontophoresis of a GABA antagonist and glutamate. *Somatosens Mot Res* 6: 109–140, 1988.

BENNETT RE, FERRINGTON DG, AND ROWE MJ. Tactile neuron classes within second somatosensory area (SII) of cat cerebral cortex. *J Neurophysiol* 43: 292–309, 1980.

BROWN AG, GORDON G, AND KAY RH. A study of single axons in the cat's medial lemniscus. *J Physiol (Lond)* 236: 225–246, 1974.

BRYSCH W, BRYSCH I, CREUTZFELDT OD, SCHLINGENSIEPEN R, AND SCHLINGENSIEPEN KH. The topology of the thalamo-cortical projections in the marmoset monkey (*Callithrix jacchus*). *Exp Brain Res* 81: 1–17, 1990.

BURTON H. Corticothalamic connections from the second somatosensory area and neighboring regions in the lateral sulcus of macaque monkeys. *Brain Res* 309: 367–372, 1984.

BURTON H. The second somatosensory cortex and related areas. In: *Cerebral Cortex. Sensory-Motor Areas and Aspects of Cortical Connectivity*, edited by Jones EG and Peters A. New York: Plenum, 1986, vol. 5, p. 31–98.

BURTON H AND JONES EG. The posterior thalamic region and its cortical projection in New World and Old World monkeys. *J Comp Neurol* 168: 249–302, 1976.

Downloaded from http://jn.physiology.org/ by 10.220.33.4 on September 27, 2016

BURTON H AND KOPF EM. Connections between the thalamus and the somatosensory areas of the anterior ectosylvian gyrus in the cat. *J Comp Neurol* 224: 173–205, 1984.

BURTON H AND ROBINSON CJ. Organization of the SII parietal cortex: multiple somatic sensory representations within and near the second somatic sensory area of cynomolgus monkeys. In: *Multiple Cortical Sensory Areas*, edited by Woolsey CN. Clifton, NJ: Humana, 1981, p. 67–119.

BURTON H AND ROBINSON CJ. Responses in the first or second somatosensory cortical area in cats during transient inactivation of the other ipsilateral area with lidocaine hydrochloride. *Somatosens Res* 4: 215–236, 1987.

BURTON H, SATHIAN K, AND SHAO DH. Altered responses to cutaneous stimuli in the second somatosensory cortex following lesions of the postcentral gyrus in infant and juvenile macaques. *J Comp Neurol* 291: 395–414, 1990.

BURTON H AND SINCLAIR RJ. Second somatosensory cortical area in macaque monkeys. I. Neuronal responses to controlled, punctate indentations of glabrous skin on the hand. *Brain Res* 520: 262–271, 1990.

BURTON H AND SINCLAIR RJ. Second somatosensory cortical area in macaque monkeys. 2. Neuronal responses to punctate vibrotactile stimulation of glabrous skin on the hand. *Brain Res* 538: 127–135, 1991.

CHMIELOWSKA J AND PONS TP. Patterns of thalamocortical degeneration after ablation of somatosensory cortex in monkeys. *J Comp Neurol* 360: 377–392, 1995.

CHUNG JM, LEE KH, SURMEIER DJ, SORKIN LS, KIM J, AND WILLIS WD. Response characteristics of neurons in the ventral posterior lateral nucleus of the monkey thalamus. *J Neurophysiol* 56: 370–390, 1986.

COLEMAN GT, ZHANG HQ, MURRAY GM, ZACHARIAH MK, AND ROWE MJ. Organization of somatosensory areas I and II in marsupial cerebral cortex: parallel processing in the possum sensory cortex. *J Neurophysiol* 81: 2316–2324, 1999.

COLEMAN GT, BAHRAMALI H, ZHANG HQ, AND ROWE MJ. Characterization of tactile afferent fibers in the hand of the marmoset monkey. *J Neurophysiol* 85: 1793–1804, 2001.

DARIAN-SMITH I, PHILLIPS G, AND RYAN RD. Functional organization in the trigeminal main sensory and rostral spinal nuclei of the cat. *J Physiol (Lond)* 168: 129–140, 1963.

DOUGLAS PR, FERRINGTON DG, AND ROWE MJ. Coding of information about tactile stimuli by neurones of the cuneate nucleus. *J Physiol (Lond)* 285: 493–513, 1978.

DYKES RW, LANDRY P, HICKS TP, DIADORI P, AND METHERATE R. Specificity of connections in the ventroposterior nuclei of the thalamus. *Prog Neurobiol* 30: 87–103, 1988.

DYKES RW, RASMUSSON DD, STRETAVAN D, AND REHMAN NB. Submodality segregation and receptive-field sequences in cuneate, gracile, and external cuneate nuclei of the cat. *J Neurophysiol* 47: 389–416, 1982.

DYKES RW, SUR M, MERZENICH MM, KAAS JH, AND NELSON RJ. Regional segregation of neurons responding to quickly adapting, slowly adapting, deep and Pacinian receptors within thalamic ventroposterior lateral and ventroposterior inferior nuclei in the squirrel monkey (*Saimiri sciureus*). *Neuroscience* 6: 1687–1692, 1981.

FERRINGTON DG AND ROWE MJ. Differential contributions to coding of cutaneous vibratory information by cortical somatosensory areas I and II. *J Neurophysiol* 43: 310–331, 1980a.

FERRINGTON DG AND ROWE MJ. Functional capacities of tactile afferent fibres in neonatal kittens. *J Physiol (Lond)* 307: 335–353, 1980b.

FISHER GR, FREEMAN B, AND ROWE MJ. Organization of parallel projections from Pacinian afferent fibers to somatosensory cortical areas I and II in the cat. *J Neurophysiol* 49: 75–97, 1983.

FRIEDMAN DP AND MURRAY EA. Thalamic connectivity of the second somatosensory area and neighboring somatosensory fields of the lateral sulcus of the macaque. *J Comp Neurol* 252: 348–373, 1986.

FULLER JH AND SCHLAG JD. Determination of antidromic excitation by the collision test: problems of interpretation. *Brain Res* 112: 283–298, 1976.

GARRAGHTY PE, FLORENCE SL, AND KAAS JH. Ablations of areas 3a and 3b of monkeys somatosensory cortex abolish cutaneous responsivity in area 1. *Brain Res* 528: 165–169, 1990a.

GARRAGHTY PE, FLORENCE SL, TENHULA WN, AND KAAS JH. Parallel thalamic activation of the first and second somatosensory areas in prosimian primates and tree shrews. *J Comp Neurol* 311: 289–299, 1991.

GARRAGHTY PE, PONS TP, AND KAAS JH. Ablations of areas 3b (SI proper) and 3a of somatosensory cortex in marmosets deactivate the second and parietal ventral somatosensory areas. *Somatosens Mot Res* 7: 125–135, 1990b.

GHOSH S, TURMAN AB, VICKERY RM, AND ROWE MJ. Responses of cat ventroposterolateral thalamic neurons to vibrotactile stimulation of forelimb footpads. *Exp Brain Res* 92: 286–298, 1992.

GOFF GD. Differential discrimination of frequency of cutaneous mechanical vibration. *J Exp Psychol* 74: 294–299, 1967.

GOLOVCHINSKY V, KRUGER L, SAPORTA SA, STEIN BE, AND YOUNG DW. Properties of velocity-mechanosensitive neurons of the cat ventrobasal thalamic nucleus with special reference to the concept of convergence. *Brain Res* 209: 355–374, 1981.

HODGKIN AL AND HUXLEY AF. The dual effect of membrane potential on sodium conductance in the giant axon of *Loligo*. *J Physiol (Lond)* 116: 497–506, 1952.

HUNT C. On the nature of vibration receptors in the hindlimb of the cat. *J Physiol (Lond)* 155: 175–186, 1961.

IGGO A AND OGAWA H. Correlative physiological and morphological studies of rapidly adapting mechanoreceptors in cat's glabrous skin. *J Physiol (Lond)* 266: 275–296, 1977.

JÄNIG W. The afferent innervation of the central pad of the cat's hind foot. *Brain Res* 28: 203–216, 1971.

JÄNIG W, SCHMIDT RF, AND ZIMMERMANN M. Single unit responses and the total afferent outflow from the cat's foot pad upon mechanical stimulation. *Exp Brain Res* 6: 100–115, 1968.

JOHANSSON RS AND VALLBO ÅB. Tactile sensory coding in the glabrous skin of the human hand. *Trends Neurosci* 6: 27–32, 1983.

JOHNSON JI. Comparative development of somatic sensory cortex. In: *Cerebral Cortex. Comparative Structure and Evolution of Cerebral Cortex*, edited by Jones EG and Peters A. New York: Plenum, 1990, vol. 8B, part II, p. 335–449.

JOHNSON JI, RUBEL EW, AND HATTON GI. Mechanosensory projections to cerebral cortex of sheep. *J Comp Neurol* 158: 81–108, 1974.

JOHNSON KO. Reconstruction of population response to a vibratory stimulus in quickly adapting mechanoreceptive afferent fiber population innervating glabrous skin of the monkey. *J Neurophysiol* 37: 48–72, 1974.

JONES EG. *The Thalamus*. New York: Plenum, 1985.

JONES EG. Connectivity of the primary sensory-motor cortex. In: *Cerebral Cortex. Sensory-Motor Areas and Aspects of Cortical Connectivity*, edited by Jones EG and Peters A. New York: Plenum, 1986, vol. 5, p. 113–183.

JONES EG AND POWELL TPS. Connections of the somatic sensory cortex of the rhesus monkey. III. Thalamic connections. *Brain* 93: 37–56, 1970.

JONES EG AND POWELL TPS. Anatomical organization of the somatosensory cortex. In: *The Handbook of Sensory Physiology. Somatosensory System*, edited by Iggo A. Berlin: Springer, 1973, vol. II, p. 263–334.

KAAS JH. The organization of neocortex in mammals: implication for theories of brain function. *Annu Rev Psychol* 38: 129–151, 1987.

KAAS JH, NELSON RJ, SUR M, DYKES RW, AND MERZENICH MM. The somatotopic organization of the ventroposterior thalamus of the squirrel monkey, *Saimiri sciureus*. *J Comp Neurol* 226: 111–140, 1984.

KARHU J AND TESCHE CD. Simultaneous early processing of sensory input in human primary (SI) and secondary (SII) somatosensory cortices. *J Neurophysiol* 81: 2017–2025, 1999.

KATZ B AND MILEDI R. A study of synaptic transmission in the absence of nerve impulses. *J Physiol (Lond)* 192: 407–436, 1967.

KRUBITZER LA AND KAAS JH. The organization and connections of somatosensory cortex in marmosets. *J Neurosci* 10: 952–974, 1990.

KRUBITZER LA AND KAAS JH. The somatosensory thalamus of monkeys: cortical connections and a redefinition of nuclei in marmosets. *J Comp Neurol* 319: 123–140, 1992.

LINDBLOM U. Properties of touch receptors in distal glabrous skin of the monkey. *J Neurophysiol* 28: 966–985, 1965.

LOE PR, WHITSEL BL, DREYER DA, AND METZ CB. Body representation in ventrobasal thalamus of macaque: a single-unit analysis. *J Neurophysiol* 40: 1339–1355, 1977.

LUX HD AND NEHER E. The equilibration time course of K_e^+ in cat cortex. *Exp Brain Res* 17: 190–205, 1973.

MACCHI G, ANGELERI F, AND GUAZZI G. Thalamo-cortical connections of the first and second somatosensory areas in the cat. *J Comp Neurol* 111: 387–405, 1959.

MACKIE PD, MORLEY JW, ZHANG HQ, MURRAY GM, AND ROWE MJ. Signalling of static and dynamic features of muscle spindle input by cuneate neurones in the cat. *J Physiol (Lond)* 510: 923–939, 1998.

MANZONI T, BARBARESI P, AND CONTI F. Anatomical and functional aspects of the associative projections from somatic area SI to SII. *Exp Brain Res* 34: 453–470, 1979.

MOUNTCASTLE VB. The neural mechanism of cognitive function can now be studied directly. *Trends Neurosci* 9: 505–508, 1986.

MOUNTCASTLE VB, TALBOT WH, SAKATA H, AND HYVÄRINEN J. Cortical neuronal mechanisms in flutter-vibration studied in unanesthetized mon-

Downloaded from http://jn.physiology.org/ by 10.220.33.4 on September 27, 2016

keys. Neuronal periodicity and frequency discrimination. *J Neurophysiol* 32: 452–484, 1969.

MURRAY GM, ZHANG HQ, KAYE AN, SINNADURAI T, CAMPBELL DH, AND ROWE MJ. Parallel processing in rabbit first (SI) and second (SII) somatosensory cortical areas: effects of reversible inactivation by cooling of SI on responses in SII. *J Neurophysiol* 68: 703–710, 1992.

NICOLELIS MAL, GHAZANFAR AA, STAMBAUGH CR, OLIVEIRA LMO, LAUBACH M, CHAPIN JK, NELSON RJ, AND KAAS JH. Simultaneous encoding of tactile information by three primate cortical areas. *Nature Neurosci* 1: 621–630, 1998.

O'MARA S, ROWE MJ, AND TARVIN RPC. Neural mechanisms in vibrotactile adaptation. *J Neurophysiol* 59: 607–621, 1988.

ORKLAND RK, NICHOLIS JG, AND KUFFLER SW. Effect of nerve impulses on the membrane potential of glial cells in the central nervous system of amphibia. *J Neurophysiol* 29: 788–806, 1966.

PONS TP. Serial processing in the somatosensory system of macaques. In: *Somesthesis and the Neurobiology of the Somatosensory Cortex,* edited by Franzén O, Johansson R, and Terenius L. Basel: Birkhäuser Verlag, 1996, p. 187–196.

PONS TP, GARRAGHTY PE, FRIEDMAN DP, AND MISHKIN M. Physiological evidence for serial processing in somatosensory cortex. *Science* 237: 417–420, 1987.

PONS TP, GARRAGHTY PE, AND MISHKIN M. Serial and parallel processing of tactual information in somatosensory cortex of rhesus monkeys. *J Neurophysiol* 68: 518–527, 1992.

PUBOLS BH AND PUBOLS LM. Coding of mechanical stimulus velocity and indentation depth by squirrel monkey and raccoon glabrous skin mechanoreceptors. *J Neurophysiol* 39: 773–787, 1976.

PUBOLS LM AND PUBOLS BH. Modality composition and functional characteristics of dorsal column mechanoreceptive afferent fibers innervating the raccoon's forepaw. *J Neurophysiol* 36: 1023–1037, 1973.

ROSE JE, BRUGGE JF, ANDERSON DJ, AND HIND JE. Phase-locked response to low-frequency tones in single fibers of the squirrel monkey. *J Neurophysiol* 30: 769–793, 1967.

ROTHENBERG M, VERRILLO RT, ZAHORIAN SA, BRACHMAN ML, AND BOLANOWSKI SJ JR. Vibrotactile frequency for encoding a speech parameter. *J Acoust Soc Am* 62: 1003–1012, 1977.

ROWE MJ. Organization of the cerebral cortex in monotremes and marsupials. In: *Cerebral Cortex. Comparative Structure and Evolution of Cerebral Cortex,* edited by Jones EG and Peters A. New York: Plenum, 1990, vol. 8B, part II, p. 263–334.

ROWE MJ, FERRINGTON DG, FISHER GR, AND FREEMAN B. Parallel processing and distributed coding for tactile vibratory information within sensory cortex. In*: Development, Organization and Processing in Somatosensory Pathways,* edited by Rowe MJ and Willis WD. New York: Liss, 1985, p. 247–258.

ROWE MJ, TURMAN AB, MURRAY GM, AND ZHANG HQ. Parallel processing in somatosensory areas I and II of the cerebral cortex. In: *Somesthesis and the Neurobiology of the Somatosensory Cortex,* edited by Franzén O, Johansson R, and Terenius L. Basel: Birkhäuser Verlag, 1996, p. 197–212.

STEPHAN H, BARON G, AND SCHWERDTFEGER WK. *The Brain of the Common Marmoset (Callithrix jacchus)—A Stereotaxic Atlas.* Berlin: Springer-Verlag, 1980.

STERIADE M, JONES EG, AND MCCORMICK DA. *Thalamus. Organization and Function.* Amsterdam: Elsevier, 1997, vol. 1.

TALBOT WH, DARIAN-SMITH I, KORNHUBER HH, AND MOUNTCASTLE VB. The sense of flutter-vibration: comparison of the human capacity with response patterns of mechanoreceptive afferents from the monkey hand. *J Neurophysiol* 31: 301–334, 1968.

TURMAN AB, FERRINGTON DG, GHOSH S, MORLEY JW, AND ROWE MJ. Parallel processing of tactile information in the cerebral cortex of the cat: effect of reversible inactivation of SI on responsiveness of SII neurons. *J Neurophysiol* 67: 411–429, 1992.

TURMAN AB, MORLEY JW, ZHANG HQ, AND ROWE MJ. Parallel processing of tactile information in cat cerebral cortex: effect of reversible inactivation of SII on SI responses. *J Neurophysiol* 73: 1063–1075, 1995.

VYSKOČIL F, KŘÍŽ N, AND BUREŠ J. Potassium selective microelectrodes used for measuring the extracellular brain potassium during spreading depression and anoxic depolarization in rats. *Brain Res* 39: 255–259, 1972.

WALDRON JN, GHOSH S, AND ZARZECKI P. Multiple inputs to a population of thalamocortical neurons projecting to cat somatosensory cortex. *Exp Brain Res* 74: 105–115, 1989.

WILSON P, KITCHENER PD, AND SNOW PJ. Cutaneous receptive field organization in the ventral posterior nucleus of the thalamus in the common marmoset. *J Neurophysiol* 82: 1865–1875, 1999.

ZHANG HQ. *Thalamocortical Somatosensory Organization in the Marmoset* (PhD thesis). Sydney, Australia: University of New South Wales, 1994.

ZHANG HQ, MURRAY GM, TURMAN AB, BAHRAMALI H, AND ROWE MJ. Parallel thalamocortical organization for tactile processing in SI and SII of the marmoset monkey: comparison of functional properties of SI- and SII-projecting thalamic neurones. *Proc Int Brain Res Organiz (IBRO). World Congr Neurosci,* 1995, p. 149.

ZHANG HQ, MURRAY GM, TURMAN AB, MACKIE PD, COLEMAN GT, AND ROWE MJ. Parallel processing in cerebral cortex of the marmoset monkey: effect of reversible SI inactivation on tactile responses in SII. *J Neurophysiol* 76: 3633–3655, 1996.

ZHANG HQ, ZACHARIAH MK, COLEMAN GT, AND ROWE MJ. Hierarchical equivalence of somatosensory areas I and II for tactile processing in the cerebral cortex of the marmoset monkey. *J Neurophysiol* 85: 1823–1835, 2001.

Downloaded from http://jn.physiology.org/ by 10.220.33.4 on September 27, 2016